Universität für Bodenkultur Wien
University of Natural Resources
and Applied Life Sciences, Vienna

MASTER THESIS

Transfer of therapy resistance in colorectal cancer cells via extracellular vesicles

submitted by
Petra Cazzanelli, BSc

carried out for the purpose of obtaining the degree of
Diplom Ingenieur

conducted at the
Comprehensive Cancer Center of the Medical University of Vienna

under the supervision of
Ao.Univ.-Prof. Dipl.-Ing. Dr. Robert Mader
Assoc. Prof. Dr. Johannes Grillari

Table of contents

Abstract

Extracellular vesicles are known to play a major role in intercellular communication and are found to be secreted by a vast number of eukaryotic cells. The high occurrence and selective cargo of extracellular vesicles in various diseases, particularly in cancer, fuelled the interest in their role in cancer development, metastasis, the influence on the tumour environment and on the development and spread of therapy resistance. Their impact on the emergence of chemoresistance against 5-fluorouracil in colorectal cancer cells was studied by co-culturing naïve primary adenoma carcinoma and lymph node metastasis cells with extracellular vesicles isolated from colorectal cancer cells with progressive degrees of chemoresistance against 5-fluorouracil followed by measurements of the EC_{50} by MTT assay. Taking into account the known impact of NF-κB on tumourigenesis, metastasis and drug resistance, its activation by extracellular vesicles isolated from the supernatant of resistant colorectal cancer cells was tested by co-cultivation and subsequent protein isolation and Western blot. The influence of several microRNAs on the NF-κB signalling pathway, was tested by transfection followed by protein isolation and Western blot. Due to the wide variability in the obtained results, no conclusion about the impact of EVs isolated from the supernatant of chemoresistant colorectal cancer cells on the chemosensitivity of naïve colorectal cancer cells could be made. Further experiments with optimized conditions and proper characterization of EVs could lead to more conclusive outcomes. Co-cultivation experiments also showed no activation of the NF-κB pathway. However, we were able to identify and validate the two miRNAs miR-301a and miR-375-3p, which were differentially expressed in chemoresistant colorectal cancer cells and are thought to have an impact on the NF-κB signaling pathway. Their role could be investigated in more detail by testing combinations of these microRNAs henceforth.

Zusammenfassung

Extrazelluläre Vesikel sind Vesikel, welche von verschiedensten eukaryotischen und prokaryotischen Zellen an ihre Umgebung abgegeben werden und eine tragende Rolle in der interzellulären Kommunikation übernehmen. Da selektiv beladene extrazelluläre Vesikel in besonders hohen Mengen in mehreren Krankheiten und vor allem bei Krebserkrankungen vorgefunden werden können, ist die Erforschung ihres Einflusses auf Krebsentwicklung, Metastasierung und Entwicklung von Therapieresistenzen von äußerstem Interesse. Die Übertragung von Therapieresistenz gegen 5-Fluorouracil in Kolonzelllinien wurde mittels Kokultivierung von naiven Kolonzelllinien mit extrazellulären Vesikeln von resistenten Kolonzelllinien und anschließender Bestimmung des EC_{50} erforscht. Der Einfluss von Kokultivierungen und von diversen microRNAs auf den NF-κB Signalweg wurde mittels Proteinisolierung und Western Blot untersucht. Aufgrund der hohen Variabilität der Ergebnisse der Kokultivierungsexperimente, konnte keine Folgerung über den Einfluss von extrazellulären Vesikeln der resistenten Zelllinien auf die Chemosensitivität von naiven Zellinien gezogen werden. Weiteres, zeigten die Kokultiverungsexperimente keine Aktivierung des NF-κB Signalwegs. Zwei miRNAs, miR-301a und miR-375-3p, welche in resistenten Kolonzelllinien differentiell exprimiert werden, wurden identifiziert und validiert. Obwohl wir keine Aktivierung des NF-κB Signalwegs nach Transfektion mit diesen miRNAs sehen konnten, kann dies durch weitere Experimente mit Kombinationen verschiedener miRNAs weiter erforscht werden.

1 Introduction

1.1 Extracellular vesicles

Extracellular vesicles, a general term describing a pool of vesicles secreted from cells to their environment, have become of growing interest in research. Even though the first indications of their existence date back to the 1970s-1980s, where the release of membrane-enclosed vesicles was described in rectal adenoma microvillus cells (De Broe et al., 1975) and a variety of mammalian cells (Trams et al., 1981), focus on extracellular vesicles in research emerged only in the recent decade as a result of new findings, which underlined their importance in intercellular communication (Yáñez-Mó et al., 2015). Furthermore, isolation from a variety of eukaryotic and prokaryotic cells, as well as from multiple body fluids demonstrated their broad occurrence, especially under cellular stress and in diseases, which fuelled further interest (Yáñez-Mó et al., 2015).

Due to their heterogeneity in content, size and membrane composition caused by different cell types, states and environments, three types of vesicles, which are summarised in the general term extracellular vesicles, have been defined: apoptotic bodies, microvesicles (MVs, also called microparticles or ectosomes) and exosomes (Figure 1). Apoptotic bodies range in size from 1 – 5 µm and are released by cells undergoing apoptosis, whereas microvesicles, sized 100 -1000 nm, are released from cells by outward budding from the plasma membrane. Lastly, exosomes are generated as intraluminal vesicles (ILVs) inside multi-vesicular endosomes (MVEs) and are released by fusion of MVEs with the plasma membrane. Their size ranges from 30 – 100 nm and is equivalent to the size of ILVs in the endosomal network. Even though their unique assembly and importance in information transfer leads to a major focus on exosomes, a lack of specific isolation and characterisation methods, as well as lacking specific markers, makes it -at present- not possible to distinguish exosomes from other extracellular vesicles, especially from MVs. Therefore, the general term extracellular vesicles is used in research, as it is of higher accuracy than the term exosomes. (Yáñez-Mó et al., 2015)

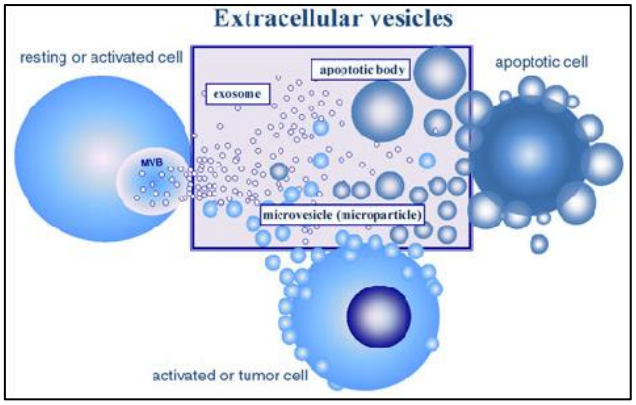

Figure 1: Subtypes of extracellular vesicles secreted from activated or apoptotic cells (Gyorgy et al., 2011)

Extracellular vesicles contain a variety of biomolecules, such as nucleic acids, proteins, lipids and sugars, packed selectively into their lipid bilayer (Figure 2). Proteins present in extracellular vesicles range from cytosolic- and cytoskeletal proteins, to membrane proteins including tetraspanins and endosome-associated proteins (Rab GTPase, SNAREs, annexxins and flottilin). The discovery of nucleic acids like DNA, messengerRNAs and microRNAs transferred selectively into extracellular vesicles led to a better comprehension of their export and influence on gene expression in cells taking up secreted EVs from their environment and led therefore to a deeper understanding of intercellular communication. These RNAs have been shown to be functional in the recipient cells affecting its function and are thought to be one of the key components in intercellular communication. Lately, also other small non-coding RNAs, like small interfering RNAs, tRNA fragments and structural RNAs were found to be components of the extracellular vesicles cargo. The membrane of extracellular vesicles was found to be enriched in sphingomyelin, cholesterol and hexosylceramides. The analysis of the composition was performed in most studies with extracellular vesicles isolated by differential centrifugation. Since this isolation method yields a mixed population of extracellular vesicles, the resulting composition analysis is not specific for different subtypes of EVs. (Raposo and Stoorvogel, 2013)

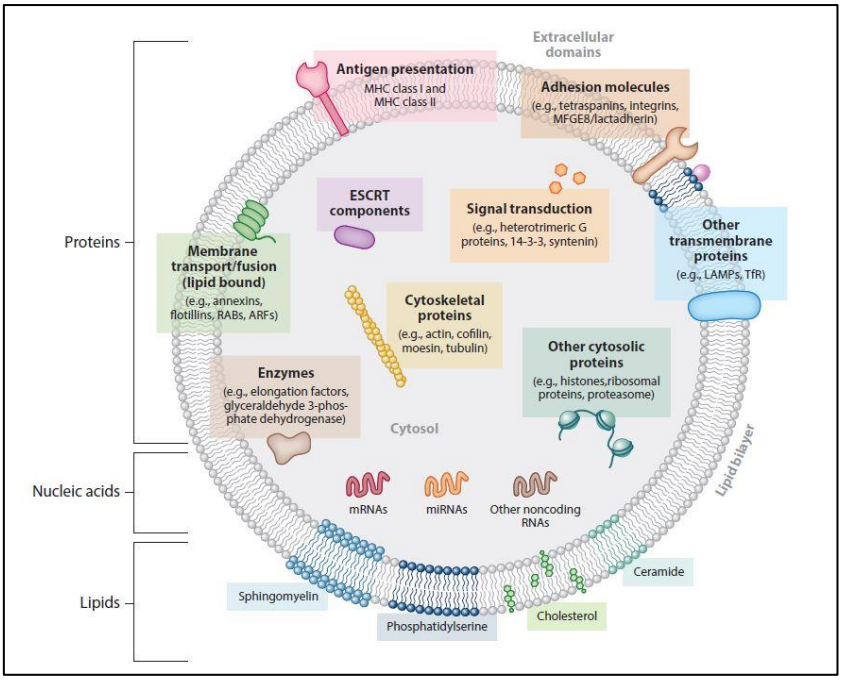

Figure 2: Composition of EVs shown as schematic representation subdivided into groups of proteins, nucleic acids and lipids.(Colombo et al., 2014)

Biogenesis and release of EVs, as well as machineries involved in these processes vary amongst the subtypes. As stated above, MVs are generated and released simultaneously by outward budding, whereas the production of exosomes involves a more complex process (Figure 3). Exosomes originate when clathrin-coated early endosomes accumulate intraluminal vesicles (ILV) in their lumen by inward budding and thereby mature into MVEs. Biomolecules involved in the MVE generation are the endosomal sorting complex required for transport (ESCRT), lipids and tetraspanins. These MVEs either go through the lysosomal pathway by fusion with lysosomes followed by degradation or turn into secretory MVEs. The latter occurs when MVE fuse with the plasma membrane and thereby secrete their ILVs, then termed exosomes. Both populations of MVEs exist simultaneously inside the cells and are sorted most probably depending on their membrane composition. (Raposo and Stoorvogel, 2013)

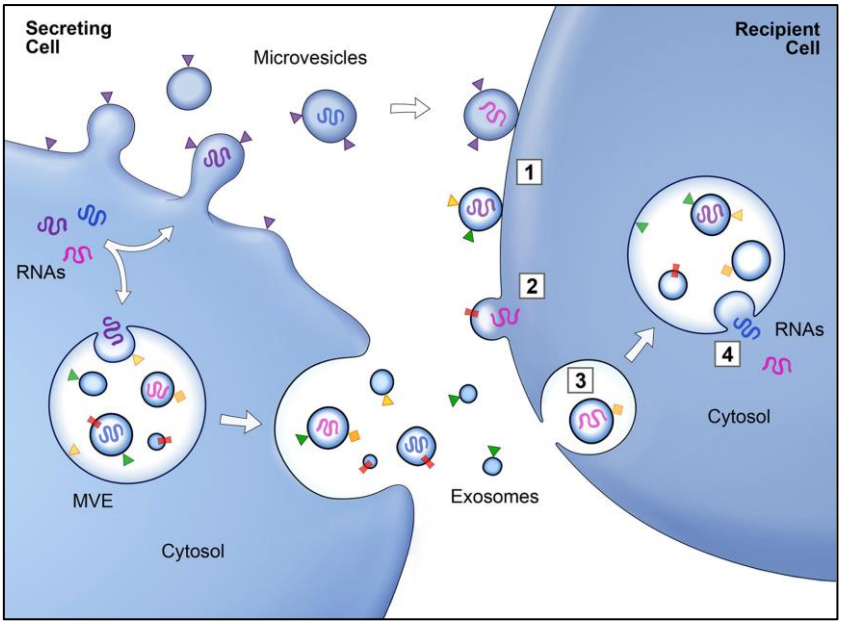

Figure 3: Intercellular communication by release of subtypes of EVs and uptake thereof by a recipient cell. Mechanisms of EV uptake: (1) docking at the plasma membrane and (2) fusion with plasma membrane; (3) endocytosis, followed by (4) fusion of the EVs with the endosomal membrane (Raposo and Stoorvogel, 2013)

The secretion of exosomes is mainly driven by the Ras-related proteins in brain (RAB) family (RAB7, RAB11, RAB27 and RAB35). On the other hand, the outward budding of plasma membrane and generation of MVs is promoted by components of the ESCRT and the ADP-ribosylation factor 6 (ARF6). (Colombo et al., 2014)

After secretion, EVs constitute a form of intercellular communication by interacting with surrounding cells. These interactions can be accomplished by juxtacrine signalling or by EV uptake. The former is based on the binding of EVs to receptors of the target cell and triggering intracellular signalling pathways. The internalization of EVs has been shown to occur by phagocytosis, clathrin- and caveolin mediated endocytosis, lipid raft-mediated endocytosis, as well as macropinocytosis. The uptake of their cargo can further result from membrane fusion. (Mulcahy et al., 2014). Once EVs or their contents are taken up by recipient cells, they were shown to influence gene expression, proteome and functions of the recipient cell, e.g. regulating immune responses or other types of pathophysiological responses (Harding et al., 2013).

1.2 Extracellular vesicles in cancer

Extracellular vesicles became of growing interest in cancer research as their potential role in cancer development, metastasis and influence on the tumour environment was discovered. Numerous studies have shown that EVs isolated from cancer cell lines and from blood plasma of cancer patients vary in their content and quantity from EVs released by healthy cells. Their cargo seems to promote angiogenesis, metastasis and immunosuppression (Cesi et al., 2016). Conditions like hypoxia, which is an important property in solid tumours like breast cancer, are known to enhance EV production and their release into the tumour microenvironment (King et al., 2012). Increased secretion of EVs triggered by hypoxia was also found in human umbilical cord derived mesenchymal stem cells promoting angiogenesis (Zhang et al., 2012). The intensified EV biogenesis was furthermore seen in melanoma patients, when the EV content was isolated from the plasma of patients and healthy donors (Logozzi et al., 2009). The unique packaging of EVs combined with their enhanced release makes them also potential biomarkers for cancer and other diseases (Niel et al., 2018).

The composition of cancer EVs compared to normal EVs is enriched in specific microRNAs and proteins and their membranes contain highly mannosylated epitopes, as well as fucosylated and sialylated epitopes and other specific lipids (Yáñez-Mó et al., 2015). This specific composition of cancer EVs and the selective packaging of microRNAs and mRNAs therein are thought to allow cancer cells to influence their microenvironment and enhance tumour progression and metastasis.

Cancer EVs have recently been identified to promote drug resistance in multiple studies (Figure 4). This was shown for example in breast cancer cells, whose survival potential was increased by incubation with EVs secreted from corresponding docetaxel-resistant lines (Chen et al., 2014). Most interestingly, the microarray data from this study showed a selective miRNA packaging in EVs from resistant cell lines. The specific subset of miRNAs in cancer EVs was also shown to impact signalling pathways and receptors of recipient cells involved in cancer progression (Challagundla et al., 2015). Furthermore, EV mediated transfer of functional efflux pumps, such as P-glycoproteins belonging to the family of ABC transporters, from resistant to sensitive human acute lymphoblastic leukaemia cells was shown by flow cytometry (Bebawy et al., 2009).

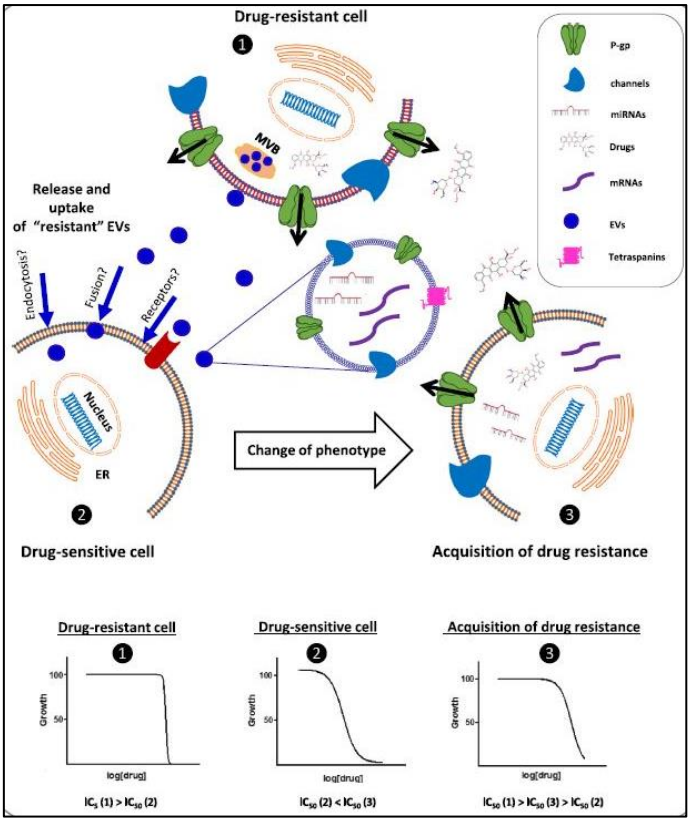

Figure 4: Emergence of drug resistance in sensitive cancer cells by uptake of EVs from resistant cancer cell lines (Cesi et al., 2016)

Enhanced secretion of EVs isolated from docetaxel resistant DU145 prostate cancer cells and their selective packaging with proteins like endophilin A2 and multidrug resistance protein (MRD) 1 and 3 was shown by Kharaziha et al., (2015). The occurrence of these selectively packaged proteins was also found in the serum of a small cohort of patients. To determine pro-metastatic properties of DU145 cells co-cultured with EVs from resistant DU145 cells, the authors performed an extracellular matrix degradation assay and were able to detect increased properties of matrix degradation. (Kharaziha et al., 2015)

1.3 Chemoresistance in colorectal cancer cells

Colorectal cancer (CRC) is a malignant tumour originating from the inner wall of the large intestine. Even though incidence rates declined annually from 2005 to 2014 by 2 - 3%, colorectal cancer is still the third most common cancer in males and females and the third deadliest cancer type. CRC incidence is declining for years due to more frequent screenings and colonoscopies, especially amongst adults over 50. The main causes for CRC are

advanced age, inappropriate diet and insufficient activity. The 5-year survival rates of patients with locally confined CRC are at 80 - 90%, those of locally advanced non metastatic tumours at 40 - 60%, whereas patients with liver metastasis have only a survival rate of 5 - 10%. (Siegel et al., 2018)

Colitis-associated CRC (CAC) is a form of CRC, which develops as a consequence of Crohn's disease or chronically active ulcerative colitis. These are two forms of inflammatory bowel diseases. CAC differs in the pathophysiology from CRC, for example in not showing an adenoma-carcinoma sequence (Fearon and Vogelstein, 1990). The typical activation of Wnt/ß-catinin pathway and adenomatous polyposis coli tumor suppressor gene in CRC, is also much rarer in CAC. On the other hand, CAC shows earlier mutations in p53 and early metastases as well as aggressive growth. (Rogler, 2014)

CRC treatment includes surgical intervention followed by chemotherapy with 5-fluorouracil (5-FU). Being an analogue of uracil, 5-FU inhibits the biosynthesis of RNAs and is converted inside the cell into fluorodeoxyuridine mono, di and triphosphate, as well as into fluorouridine triphosphate (FUTP). Understanding intracellular processes linked to 5-FU administration is essential for the elucidation of the developing chemoresistance in treated cells. (Longley et al., 2003)

Development of drug resistances, for example against 5-FU, in cancer treatment is one of the major challenges for cancer research, since most successful cancer therapies fail after long-term exposure (Schmidt et al., 2004). The onset of resistances is considered as a complex process fuelled by drug compartmentalisation, drug efflux and decreased accumulation, as well as intercellular genetic modifications of drug targets and pathways (Vadlapatla et al., 2013).

1.4 NF-κB signalling pathway and miRNA

Inducible transcription factors, like the nuclear factor κB (NF-κB), are essential tools for mammalian cells to adapt and respond to environmental conditions by flexible regulation of their gene expression. The NF-κB signalling pathway is triggered by extracellular stimuli, which lead to a number of subsequent reactions like protein phosphorylation, deactivation and degradation of physiological NF-κB inhibitors, finally resulting in the translocation of the central NF-κB molecule p65 into the nucleus, where it can regulate gene expression. This pathway is known to play a crucial role in the cellular immune response influencing cell survival,

differentiation and proliferation after its activation. Having such a broad impact on numerous cellular processes, the dysregulation of NF-κB leads to serious consequences and is found in various pathological conditions like cancer and inflammatory diseases. (Hayden and Ghosh, 2008)

The canonical NF-κB signalling pathway consists of three major groups of proteins: IKK, IκB and NF-κB/Rel proteins. The NF-κB/reticuloendotheliosis (Rel) protein dimers can be translocated from the cytosol into the nucleus, where they bind to the DNA motif κB. Proteins inhibiting NF-κB/Rel are called IκB (inhibitor of NF-κB) and consist of IκBα, IκBβ, IκBε, IκBγ and BcI-3. The kinase responsible for the phosphorylation of IκB proteins are called IKK. This multiprotein kinase consists of two catalytic subunits (IKKα and IKKβ) and a regulatory subunit (IKKγ, also called NEMO). Under normal circumstances, the pathway is inactive and NF-κB is bound to its inhibitor IκB. NF-κB is activated either by the canonical or the alternative pathway (Figure 5).The activation is triggered by environmental stimuli binding to cell-surface receptors like T-cell and B-cell receptors (TCR/BCR), toll like receptors (TLRs), tumour necrosis factor receptors (TNFα, CD40) and the receptor activator of NF-κB (RANK). Focusing on the canonical pathway, this leads first to the activation of IKK by phosphorylation. Activated IKK phorphorylates IκB proteins, which then dissociate from the NF-κB/Rel complex and therefore release NF-κB. After release, NF-κB dimers are translocated into the nucleus. The proteolytic degradation of phosphorylated IκB proteins is induced by polyubiquitinylation thereof. (Jost and Ruland, 2007)

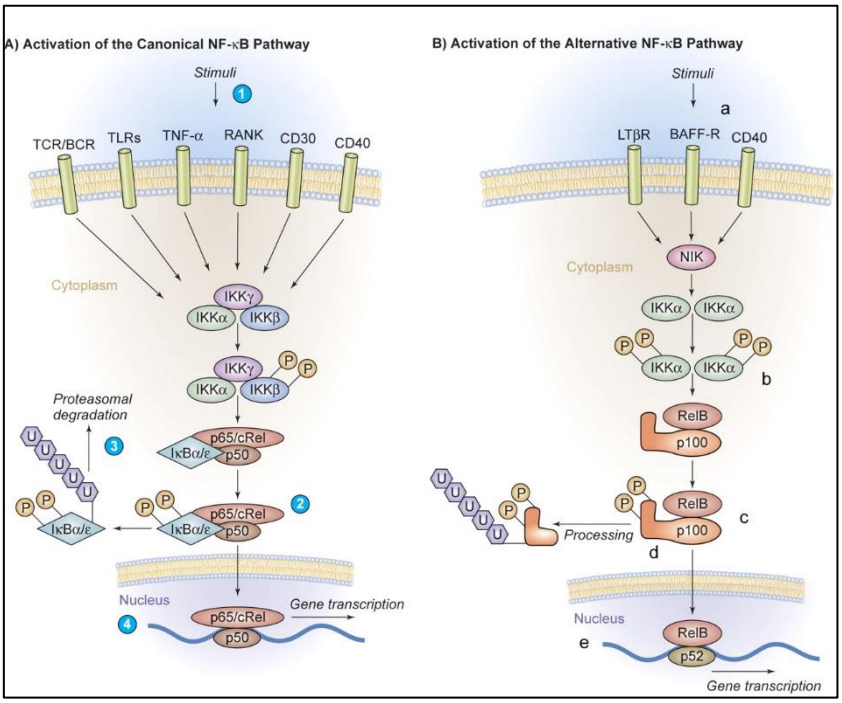

Figure 5: The canonical and alternative NF-κB signaling pathway (Jost and Ruland, 2007)

The NF-κB signalling pathway was first found to be an essential player in immunity and inflammation and is involved in cell proliferation and apoptosis. These processes are also known to be linked to tumour development and progression. Therefore, the importance of NF-κB and its dysregulation in cancer became of emerging interest (Viatour et al., 2005). It was also shown, that the pathway can be activated by many oncogenes and is linked closely to tumourgenesis (Bharti and Aggarwal, 2002). Since the activation of NF-κB was observed in numerous cancer types like breast and leukaemia cancer cells and elevated levels seem to correlate with poor prognostic outcomes, this pathway has become of great interest as a novel drug target. Inhibition of the activity of NF-κB with the soy isoflavone genistein in prostate, breast, lung and pancreatic cancer cells resulted in increased growth inhibition and apoptosis induced by chemotherapeutic agents (Li et al., 2005). Additionally, NF-κB activation was determined as an important mechanism in the development of resistance against chemotherapies like cisplatin (Godwin et al., 2013).

As modulators of NF-kB expression, small non coding RNAs like microRNAs are known to have an impact on cancer initiation and progression, but also on immune responses and inflammation. Therefore, examination of the impact of miRNAs on the NF-κB signalling pathway has become of growing interest. Comparing miRNA targets with genetic targets of this transcription factor may lead to a deeper understanding of the link between cancer, microRNAs and the dysregulation of the NF-κB pathway (Ma et al., 2011). Several miRNAs were found to be regulatory components of the NF-κB pathway. The miRNAs miRNA-181b, miR-21, miR-146, miR-155 and miR-301a were described for their impact on the pathway by Ma et al (2011). A study by Olarerin-George et al (2013) highlighted the importance of miR-125, miR-141and miR-517 as activators and miR-375 as repressor of NF-κB. The miR-125b was not only connected to NF-κB, but also to tumorgenesis in skin cancer (Tan et al., 2012). Another family of microRNAs, the miR-200 family, which is intensely studied in cancer development, therapy resistance and metastasis, is also known to coordinate signalling cascades like the NF-κB pathway (Mutlu et al., 2016). The loss of exosomal miR-200c in chemoresistant colorectal cancer cell lines was shown to enhance in vitro invasiveness by de-repressing EMT-regulating transcription factors ZEB1 and SLUG (Senfter et al., 2015).

1.5 Aim of the study

In the past decades, extracellular vesicles have become an important research topic in many diseases, particularly in cancer research, because of their emerging role in intercellular communication. Focusing on the emergence of therapy resistances in cancer treatment, extracellular vesicles and the transfer thereof might explain the development and spread of drug resistance amongst cancer cells. The aim of this study was to shed further light on the development of chemoresistance against 5-fluorouracil in colorectal cancer cells, by coculturing naïve primary adenoma carcinoma and lymph node metastasis cells with extracellular vesicles isolated from colorectal cancer cells with progressive degrees of chemoresistance against 5-fluorouracil. Taking into account the suggested impact of NF-κB on tumourigenesis, progression, metastasis and drug resistance, its activation by extracellular vesicles was of further interest, as well as the influence of microRNAs on the pathway.

Based on this background knowledge, following hypotheses were studied:

1) Do extracellular vesicles isolated from the supernatant of resistant colorectal cancer cells have an impact on the chemosensitivity of naive primary adenoma carcinoma cells and of naive lymph node metastasis cells?
2) Do extracellular vesicles isolated from the supernatant of resistant colorectal cancer cells have an impact on the NF-κB signalling pathway of naive lymph node metastasis cells?
3) Does the transfection of naive lymph node metastasis cells with microRNAs, which are differentially expressed in naïve and resistant cancer cells and which are known to influence the NF-κB signalling pathway, lead to the activation thereof?

2 Materials and Methods

2.1 Cell culture

The impact of extracellular vesicles on resistance, activation of the NF-κB pathway and their miRNA content was analysed in various colorectal cancer cell lines, including the naïve primary adenoma carcinoma cell line CCL 228 (also called SW480), its lymph node metastasis CCL 227 (SW620) with progressive degrees of chemoresistance against 5-fluorouracil, as well as the colorectal carcinoma cell line CCL 247 and another adenoma carcinoma cell line CaCo2. The CCL 228 cell line originates more specifically from Dukes' type B colorectal adenoma carcinoma and CCL 227 from Dukes' type C colorectal adenoma carcinoma. All cell lines, except from the resistant ones, where obtained from the American Type Culture Collection (Rockville, MD, USA). The chemoresistant cell lines were established previously by continuous exposure of CCL 227 cells to different concentrations of 5-fluorouracil (Mader et al., 1997). The cell lines used for all following experiments are listed in Table 1.

Table 1: Characteristics of colorectal cancer cell lines used for experiments

CELL LINE		5-FU RESISTANCE
CCL 228	naive primary adenoma carcinoma cell line	0 µM
CCL 227	naive lymph node metastasis cell line	0 µM
CCL 227 + 5 µM 5-FU	low resistant lymph node metastasis cell line	5 µM
CCL 227 + 25 µM 5-FU	intermediate resistant lymph node metastasis cell line	25 µM
CCL 227 + 125 µM 5-FU	high resistant lymph node metastasis cell line	125 µM
CCL 247	primary colorectal carcinoma	0 µM
CaCo2	epithelial adenoma carcinoma cell	0 µM

2.1.1 Cultivation of colorectal cancer cells

Materials

- T75 or T125 flasks (Corning®, Sigma-Aldrich)
- RPMI Medium 1640 (1x) + GlutaMAX™ (GIBCO®, Thermo Fisher Scientific)
- Fetal Bovine Serum (w/o extracellular vesicles) (Sigma-Aldrich)
- Accutase® solution for cell culture (Sigma-Aldrich)
- DPBS (1x) (GIBCO®, Thermo Fisher Scientific)

Procedure

Cells were cultivated in T75 or T125 flasks with RPMI 1640 containing GlutaMAX™ and 10% fetal bovine serum (FBS) in a humidified atmosphere at 37°C and 5% CO_2. Chemoresistant cells were cultivated in RPMI 1640 containing GlutaMAX™, 10 % FBS and adequate concentrations of 5 µM, 25 µM or 125 µM of 5-fluorouracil dissolved and diluted in 0.9% NaCl. For some experiments, FBS was depleted from extracellular vesicles and other impurities before being added to the media. This was achieved by differential centrifugation and sterile filtration. The cells were cultivated to a confluence of 80% and split twice a week. To split cells, the medium was removed and the cells were carefully washed twice with DPBS. For the detachment of the cells from the surface, they were incubated for 5 minutes at 37°C with 2 mL or 5 mL accutase respectively. Afterwards the cells were recovered in RPMI 1640 + GlutaMAX™ + 10% FBS, centrifuged for 5 minutes at 287 g and resuspended again in RPMI medium. An adequate amount of cell suspension was then transferred back to the flasks and cultivated further in a humidified atmosphere at 37°C and 5% CO_2.

2.2 Isolation of extracellular vesicles from cell culture supernatant

Enrichment of extracellular vesicles from conditioned cell culture medium was achieved either by precipitation with polyethylene glycol or by two differential centrifugations and a subsequent ultracentrifugation step. Precipitation was used for the first set of experiments, as well as for experiments where large amounts of extracellular vesicles were needed, since it is less time and cost intensive than differential centrifugation. Both methods are described below (see 2.2.1 and 2.2.2) in more detail. However, differential centrifugation is the more precise and most widely used isolation technique (Gardiner et al., 2016).

2.2.1 Isolation of extracellular vesicles with polyethylene glycol

Extracellular vesicles were isolated for certain experiments from conditioned cell culture medium by precipitation of the extracellular vesicles with the volume-excluding polymer polyethylene glycol (PEG). (Vlassov et al., 2013)

Materials

- PEG 6000 (30% w/v) (Sigma-Aldrich)
- DPBS (1x) (GIBCO®, Thermo Fisher Scientific)
- 15 mL centrifuge tubes (Corning®, Sigma-Aldrich)

Procedure

Cells were cultivated for 48 h in RPMI Medium 1640 + GlutaMAX™ + 10% FBS w/o extracellular vesicles to a confluence of around 80%. The supernatant was then harvested and centrifuged at 2000 g for 30 minutes at 4°C to discard cell debris. Afterwards 5 mL of supernatant was mixed with 2.5 mL PEG 6000 (30% w/v) and incubated overnight at 4°C. On the next day the supernatant-PEG mixture was centrifuged for 1 h at 10000 g and 4°C. The pellet containing the precipitated extracellular vesicles was resuspended in 100 µL DPBS.

2.2.2 Isolation of extracellular vesicles with differential centrifugation

Differential centrifugation is nowadays the most common method to isolate extracellular vesicles from conditioned media (Gardiner et al., 2016). Density gradients are used to separate unwanted fractions from conditioned media and finally enrich extracellular vesicles. Particles, which are larger in size and denser, are sedimented at lower g forces. Therefore, multiple steps of centrifugation at increasing g forces are used to first remove cells, dead cells and cell debris, as well as apoptotic bodies. These first steps are followed by a final step of ultracentrifugation at very high g forces – above 100000 g – where extracellular vesicles are sedimented.(Thery et al., 2006)

Materials

- DPBS (1x) (GIBCO®, Thermo Fisher Scientific)
- 50 mL centrifuge tubes (Corning®, Sigma-Aldrich)
- sterile syringe filter, 0.22 µm pore size (Merck)
- 5 mL polypropylene tubes for UZ (Beckman Coulter)

Procedure

Extracellular vesicles were purified by collecting the supernatants of cells cultivated for 48 h in RPMI Medium 1640 + GlutaMAX™ + 10% FBS w/o extracellular vesicles. The conditioned media was first centrifuged for 10 minutes at 500 g and then for 15 minutes at 14000 g to sediment cell debris. These two centrifugation steps were followed by a filtration step with a 0.22 µM syringe filter to eliminate a fraction of apoptotic bodies. The media was then centrifuged at 120000 g for 70 minutes to sediment extracellular vesicles. After discarding the supernatant very carefully, the pellet was resuspended in DPBS.

2.2.3 Concentration measurement of extracellular vesicles

Total protein concentrations of the isolated samples were measured with the Bradford Protein Assay (BioRad). This is a colorimetric assay, where a shift in the absorbance maximum is measured due to the binding of Coomassie Brilliant Blue G-250 to the proteins in solution. The dye has an usual absorbance maximum of 465 nm, but after it reacts with proteins in the probe, this absorbance maximum shifts to 595 nm. By measuring this shift against a standard curve, it is possible to determine the protein concentration with the Lambert-Beer law. (Bradford, 1976)

Materials

- Bovine serum albumin (BSA) standard (BioRad)
- Protein assay dye reagent concentrate (BioRad)
- H_2O_{dd}
- sterile syringe filter, 0.22 µm pore size (Merck)
- 96 well plate

Procedure

For the standard curve, a BSA standard with a stock concentration of 1.45 mg/mL was diluted to concentrations of 0.050 mg/mL (ST1), 0.075 mg/mL (ST2), 0.100 mg/mL (ST3), 0.200 mg/mL (ST4), 0.400 mg/mL (ST5), 0.500 mg/mL (ST6) with H_2O_{dd}. The dye reagent concentrate was also diluted 1:5 and filtrated through a 0.22 µm sterile syringe filter. The extracellular vesicles isolated with PEG 6000 were diluted 1:50 and those isolated with differential centrifugation 1:10. Then 10 µL of each standard dilution and the probes were pipetted into a 96 well plate and 200 µL dye reagent were added to each of them. After 5 minutes of incubation, the standards and probes were measured with the ELISA reader Asys Expert Plus at a wavelength of 595 nm. All samples were measured in duplicates.

2.3 Cell Culture Assays

2.3.1 MTT Assay

The MTT assay is a colorimetric cell viability assay to determine the number of viable cells in multiwell plates. MTT, 3-(4,5-dimethylthiazol-2-yl)-2,5-diphenyltetrazolium bromide, is a tetrazolium dye, which is positively charged and can therefore penetrate the membrane of eukaryotic cells. Viable cells then reduce the tetrazolium to purple coloured formazan, which has an absorbance maximum at 570 nm. Changes in the absorbance at 570 nm can be measured with a plate reading spectrophotometer. Although the exact mechanism of MTT reduction by cells is not yet understood completely, it is assumed that NADH or other reducing molecules are involved in the electron transfer. (Riss et al., 2013)

The effective concentration (EC_{50}) of a cytotoxic agent like 5-fluorouracil can be determined with the MTT assay by measuring the absorbance of cells exposed to a logarithmic dilution series of 5-fluorouracil. Plotting the absorbance at 570 nm against the logarithm of the concentration of the cytotoxic agent and fitting the curve using nonlinear regression curve fit results in a sigmoidal dose-response curve, by means of which the EC_{50} can be calculated.

Various MTT assays were performed with naïve and chemoresistant cell lines incubated with varying amounts of extracellular vesicles.

Materials

- 60 mM 5-fluorouracil
- DPBS (1x) (GIBCO®, Thermo Fisher Scientific)
- 98% MTT (Sigma-Aldrich) salt solution in DPBS (GIBCO®, Thermo Fisher Scientific)
- Solubilization solution (40% N,N-Dimethylformamid, 20% SDS; adjusted to pH-value of 4.5 - 5 with CH_3COOH)
- RPMI Medium 1640 + GlutaMAX™ (GIBCO®, Thermo Fisher Scientific)
- Fetal Bovine Serum (w/o extracellular vesicles) (Sigma-Aldrich)
- 96 well plates

Procedure

Cells were incubated in triplets in 96 well plates (á 5000 cells/well, in a total volume of 100 µL) for 24 hours at 37°C and 5% CO_2. For the determination of the exact cell count/mL, the viable cells were counted with Bürker – Türk counting chambers. After 24 h of incubation in cell culture medium, 25 µL of the cytostatic 5-fluorouracil dilution series was added to the cells. The 5-FU 60 mM stock solution was diluted in DPBS in a decimal series of dilutions from 60 mM to 60 nM, which then led to final concentrations of 10 mM to 10 nM in the wells (25 µL of the primary 5-FU dilution in 150 µL total volume equates to a 1:6 dilution). After 6 days 15 µL MTT dye solution were added and the cells were incubated for 4 h at 37°C and 5% CO_2. To solubilize the precipitated formazan, 100 µL solubilisation solution were added after 4 h and the cells were then incubated for another 24 h at room temperature. The measurement was done with the Biochrom Asys Expert Plus Microplate Reader: extinction 570 nm, reference wavelength 690 nm. The data was then analysed with GraphPadPrism 4.0 program with nonlinear regression curve fitting resulting in a sigmoidal dose-response curve.

2.3.2 PDT Assay

Population doubling time assays (PDT) give an understanding of the doubling time of cells and can show the impact of substances added to cells on their growth and viability. Cells were incubated with extracellular vesicles from chemoresistant cell lines and by addition of MTT (description see chapter 2.3.1 MTT Assay) and measurement of cell viability at 5 different time points (24 h, 48 h, 72 h, 100 h, 168 h), the population doubling time could be calculated.

Material

- 60 mM 5-Fluorouracil
- DPBS (1x) (GIBCO®, Thermo Fisher Scientific)
- 98% MTT (Sigma-Aldrich) salt solution in DPBS (GIBCO®, Thermo Fisher Scientific)
- Solubilization solution (40% N,N-Dimethylformamid, 20% SDS; adjusted to pH-value of 4.5-5 with CH_3COOH)
- RPMI Medium 1640 + GlutaMAX™ (GIBCO®, Thermo Fisher Scientific)
- Fetal Bovine Serum (w/o extracellular vesicles) (Sigma-Aldrich)
- 96 well plates

Procedure

Cells were incubated in triplets in five (for each time point) 96 well plates (á 5000 cells/well, in a total volume of 150 µL) for 24 h at 37 °C and 5% CO_2. For the determination of the exact cell count/mL, the viable cells were counted with Bürker – Türk counting chambers. Extracellular vesicles isolated from the cell lines CCL 227 + 5µM 5-FU, CCL 227 + 25µM 5-FU or CCL 227 + 125µM 5-FU were added to the cells. At 5 consecutive time points (24 h, 48 h, 72 h, 100 h, 168 h) 15 µL MTT salt solution were added to each well. After a 4 h incubation period at 37°C and 5% CO_2, 100 µL of solubilisation solution were added and another incubation period of 24 hours at room temperature followed. Measurement of each plate was carried out by Biochrom Asys Expert Plus Microplate Reader (extinction 570 nm, reference wavelength 690 nm). The data was analyzed with the GraphPadPrism 4.0 program by plotting the measured extinction against the time periods. The slope of the resulting curve (m) was used to calculate the population doubling time according to Equation 1.

$$\boldsymbol{PDT} = \frac{\log 2}{\boldsymbol{m}} \qquad \text{Equation 1}$$

2.4 NF-κB signalling pathway kinetics

For NF-κB kinetics, CCL 227 cells were incubated with varying amounts of extracellular vesicles from resistant cell lines and harvested at different time points. Activation of the NF-κB signalling pathway was then analysed by Western blotting against IKKα, IKKβ, IκBα, p65 and their phosphorylated forms phospho-IKKα/IKKβ, phospho-IκBα and phospho-p65.

2.4.1 Incubation of cells with extracellular vesicles and cell lysis

Cell lysis is an essential step to extract the total protein amount of cells: Protein extracts can then be analysed further to identify specific proteins of interest by Western blotting. To obtain the total protein content of the cell cytosol and to avoid protein degradation or modification, the addition of protease and phosphatase inhibitors during cell lysis is essential. Furthermore, comparability of different samples must be guaranteed by determining the concentration and dilution to get a comparison on equivalent basis. (Mahmood and Yang, 2012)

Materials

- CCL 227 cell line
- CCL 227 + 125 µM 5-FU cell line
- RPMI Medium 1640 + GlutaMAX™ (GIBCO®, Thermo Fisher Scientific)
- Fetal Bovine Serum (w/o extracellular vesicles) (Sigma-Aldrich)
- Extracellular vesicles isolated from CCL 227 + 125 µM 5-FU cell line with PEG or UZ isolation
- DPBS (1x) (GIBCO®, Thermo Fisher Scientific)
- 2x SDS lysis buffer (pH 6.8; containing: 0.5 M Tris-HCL, 20% SDS, 100% glycerine (Merck), 0.5 M EDTA (Sigma), PhosphoSTOP phosphatase inhibitor cocktail (Roche),complete mini EDTA-free protease inhibitor cocktail (Roche))
- ddH20

Procedure

Naïve lymph node metastasis cells CCL 227 were incubated with extracellular vesicles isolated from the high resistant cell line CCL 227 + 125 µM 5-FU. The cells were harvested at a confluence of 80% from one T75 flask, resuspended in 3 mL RPMI Medium 1640 +

GlutaMAX™ + 10% FBS w/o extracellular vesicles and seeded at a ratio of 1/10 per 25 cm^2 flask = 300 µL cell suspension in 5 mL cell culture medium. The experimental set up is shown in Table 2. Cells were incubated at 37°C, 5% CO2 for 24h.

Table 2: Experimental set up for NF-κB kinetics

FLASK	CELL LINE	EXTRACELLULAR VESICLES	INCUBATION TIME
1st flask	CCL227+125 µM 5-FU	-	0 h
2nd flask	CCL 227	-	0 h
3rd flask	CCL227	-	1 h
4th flask	CCL 227	+ EV from CCL227 + 125 µM 5-FU	1 h
5th flask	CCL 227	-	4 h
6th flask	CCL227	+ EV from CCL227 + 125 µM 5-FU	4 h
7th flask	CCL 227	-	24 h
8th flask	CCL 227	+ EV from CCL227 + 125 µM 5-FU	24 h

After 24 h the media was changed and different amounts of EV per flask were added. After 0 h – 1 h – 4 h – 24 h the supernatant of the respective flasks was removed, the cells were washed two times with cold DPBS and lysed with 50 µL 2x SDS-lysis buffer. Than the cells were detached with a cell scraper, transferred into tubes and sonicated with 10-15 pulses. The protein concentration was measured against aqua destillata using a spectrophotometer (Hitachi - U-2900). For this purpose, each sample was diluted 1:100 with ddH_2O and concentrations were calculated via extinction: E 0.1 = 1.3 µg/µL.

2.4.2 SDS PAGE

Sodium dodecyl sulfate - polyacrylamide gelelectrophoresis, short SDS-PAGE, is a method used for separation of protein extracts, which were obtained by cell lysis. Negatively charged and previously denatured proteins are separated according to their molecular weight in a gel matrix by applying an electric field. The gel matrix consists of an upper 4% acrylamide/bis stacking gel with a porous structure, which is used to define a sharp band, and a lower 10% acrylamide/bis separating gel with a defined and denser pore size, which is used for the separation of the proteins according to their size. Proteins, being negatively charged, travel toward the positive electrode, when voltage is applied. Smaller proteins travelling more easily

and therefore faster through the pores can be separated from larger proteins, which take more time. By comparison of the bands with the protein standard, the size of the proteins can be determined. (Mahmood and Yang, 2012)

Materials

- Solutions listed in Table 3
- Precision Plus Protein Dual Color Standard (Bio-Rad)
- Composition of gels shown in Table 4 and Table 5

Table 3: Solutions for SDS-PAGE

SOLUTION	PREPARATION
5x Tris-glycine buffer	125 mM tris(hydroxymethyl)aminomethane (Tris-base) (Merck) 1.250 M Glycine (Merck) 0.5% SDS (Pharmacia) dissolved in 1 L ddH2O, pH 8.3 (adjusted with HCL), stored at RT. 1x Tris-glycine buffer was used for gel electrophoresis
2x Sample buffer	72 mM 1,4 Dithiothreitol (DTT) (Merck) dissolved in 5 ml ddH2O, 5 ml 100% glycerine (Merck) and a tip bromphenol blue (Merck) were added. 200 µl aliquots were stored at -20°C.
1 M Tris-HCl	1 M Tris-base (Merck) dissolved in 100 mL ddH2O, pH 9.1 (adjusted with HCL), stored at RT
0.5 M Tris-HCl	0.5 M Tris-base (Merck) dissolved in 100 mL ddH2O, pH 6.8 (adjusted with HCL), stored at RT
10% SDS	Sodiumdodecylsulfate (Pharmacia) dissolved in 100 mL ddH2O, filtered and stored at RT.
40% APS	Ammonium peroxodisulfate (Fluka) dissolved in 1 mL ddH2O and stored in aliquots at -20°C.
Temed	BioRad

Table 4: Composition of separating gel (10 % acrylamid/bis)

REAGENTS	VOLUME
Acrylamide/bis 30%	1.5 mL
ddH_2O	1.5 mL
1 M Tris-HCl (pH=9.1)	1.9 mL
10% SDS	50 µL
40% APS	10 µL
Temed	2.5 µL

Table 5: Composition of stacking gel (4 % acrylamid/bis)

REAGENTS	VOLUME
Acrylamide/bis 30%	0.325 mL
ddH_2O	0.625 mL
1 M Tris-HCl (pH=9.1)	1.55 mL
10% SDS	25 µL
40% APS	4 µL
Temed	2.5 µL

Procedure

For SDS PAGE 10 µg of cellular protein lysate were substituted to a volume of 10 µL with 1x tris-glycine buffer (final concentration of protein lysate: 1 µg/µL). After addition of 10 µL 2x sample buffer, the samples were denatured for 3 minutes at 99.99°C. Gels were prepared sequentially, first casting the separating gel and then the stacking gel. Each sample (20 µL) as well as 5 µL of protein marker were loaded onto the gel and the gels were run in a BioRad chamber with 1x tris-glycine buffer at 150 V for around 60 minutes.

For each NF-κB kinetic performed, a total number of 10 gels had to be run. These 10 gels were needed for subsequent Western blot analysis of IKKα, IKKβ, phospho-IKKα/ IKKβ, IκBα, phospho-IκBα, p65 and phospho-p65 enzymes as well as the housekeeping gene glyceraldehyde 3-phosphate dehydrogenase (GAPDH), which served as control at each plotting session.

2.4.3 Western blot

Western blotting is a technique used to identify specific proteins of interest from the total protein content of cell lysates. After separation of proteins according to their molecular weight by SDS-PAGE and transfer thereof onto a PVDF membrane by a semi-dry electrophoretic transfer, proteins of interest can be identified by incubation with primary and secondary antibodies binding specifically to these proteins. Target proteins are then detected by chemiluminescence detection. Exposing membranes to luminol/enhancer solution and stable peroxide solution, a signal can be detected corresponding to the position of the proteins. This signal can be captured on a Hyperfilm™ ECL film and developed in a dark room. (Mahmood and Yang, 2012)

Materials

- Solutions for Western blot listed in Table 6
- Whatman® paper (Thermo Scientific)
- PVDF membrane (0.45 µM, Thermo Scientific)
- Hyperfilm™ ECL (GE Healthcare)

Table 6: Solutions for western blot analysis

SOLUTION	PREPARATION
Transfer buffer	39 mM glycine, 48 mM Tris-base, 0.037% SDS (Pharmacia) and 20% methanol (Merck) dissolved and filled up with ddH2O to 1 L, filtered and stored at 4°C
10x Tris buffered Saline (TBS)	136.9 mM NaCl (Merck), 5.4 mM KCl (Merck) and 49.5 mM Tris-base (Merck) dissolved in 1 L ddH2O, pH 7.4 (adjusted with HCL), after filtration stored at RT. 1x TBS was used for gel electrophoresis
SuperBlock Blocking Buffer in TBS	Thermo Scientific
Tween 20	0.5 M Tris-base (Merck) dissolved in 100 mL ddH2O, pH 6.8 (adjusted with HCL), stored at RT
Super Signal West Dura Extended	Thermo Scientific

Procedure

Proteins were transferred from the acrylamide gels to transfer membranes via semi-dry membrane transfer. The transfer was set up as follows: positive electrode – Whatman® paper (conditioned in transfer buffer) – PVDF transfer membrane (conditioned first in methanol then in transfer buffer) – gel (conditioned in transfer buffer) – Whatman® paper (conditioned in transfer buffer) – negative electrode for 1 h at 0.8 mA/cm^2 membrane (5-8V). The transferred proteins were then blocked on the membrane with 15 mL SuperBlock blocking buffer in TBS with 0.05% Tween 20 overnight at 4°C. Blocked membranes were then incubated for one hour at room temperature with primary antibodies (listed in Table 7), washed 5 times for 10 minutes with 1x TBS with 0.05% Tween 20 and incubated thereafter one hour with secondary antibodies (listed in Table 8) at room temperature. After another washing step (5 times for 10 minutes with 1x TBS with 0.05% Tween 20), membranes were incubated 5 minutes with 2.5 mL stable peroxide solution and 2.5 mL luminol/enhancer solution. High performance chemiluminescence Amersham Hyperfilm™ ECL (GE Healthcare) was then exposed to the transfer membranes and developed in the developer Agfa Curix 60. Exposure time was varied to obtain the ideal signal intensity.

Table 7: Primary antibodies used for Western blot analysis

Antibody	Dilution	2nd Antibody	Molecular weight (kDa)	Company	Serial number
IKKα	1 : 2000	anti-mouse	85	Cell Signalling Technology	3G12
IKKβ	1 : 2000	anti-rabbit	87		D30C6
Phospho-IKKα/β	1 : 2000	anti-rabbit	85 (IKKα) 87 (IKKβ)		16A6
NF-κB p65	1 : 1000	anti-rabbit	65		D14E12
Phospho-NF-κB p65	1 : 1000	anti-rabbit	65		93H1
IκBα	1 : 2000	anti-mouse	39		L35A5
Phospho-IκBα	1 : 2000	anti-rabbit	40		14D4
GAPDH	1 : 5000	anti-rabbit	37	Santa Cruz	**sc-25778**

Table 8: Secondary antibodies used for western blot analysis

ANTIBODY	DILUTION	COMPANY
Goat anti-mouse IgG (peroxidase conjugated)	1:100000	Thermo Scientific
Goat anti-rabbit IgG (peroxidase conjugated)	1:100000	Thermo Scientific

2.5 Transfection of cells with miRNA

Transfection is a method to introduce transiently or stably foreign nucleic acids like DNA, mRNA or miRNA into mammalian cells. This can be achieved biologically by transfecting cells with viruses containing the foreign DNA, physically by electroporation or direct injection or chemically with cationic polymers, calcium phosphate or cationic lipids. Chemical transfection procedures are among the most widely used and were also the method of choice for the following transfection experiments. In principle, positively charged chemicals form a complex with the negatively charged nucleic acids. These lipid-nucleic acid complexes are then taken up by the cells presumably by phagocytosis and endocytosis. (Kim and Eberwine, 2010)

Transfection of the naive lymph node metastasis cell line CCL 227 with miR-301 mimic and miR-375 mimic was performed by cationic lipids based transfection. After transfection, cells were lysed, their proteins extracted and analysed by Western blot. Transcription levels of miR-301 and miR-375 were determined by quantitative real time PCR.

Material

- HiPerFect Transfection Reagent (Qiagen)
- miScript miR-301 mimic (Qiagen) Stock: 20 µM
- miScript miR-375 mimic (Qiagen) Stock: 20 µM
- Negative control siRNA (Qiagen) Stock: 20 µM
- RPMI Medium 1640 + GlutaMAX™ (GIBCO®, Thermo Fisher Scientific)
- T75 flasks (Corning®, Sigma-Aldrich)

Experimental set up

Table 9: Experimental set up for miRNA transfection

SAMPLES FOR RT-PCR			SAMPLES FOR WESTERN BLOT		
1st	CCL227	+ miR301 mimic	1st	CCL227	+ miR301 mimic
2nd		+ miR375 mimic	2nd		+ miR375 mimic
3rd		+ neg. control siRNA	3rd		+ neg. control siRNA
4th	CCL227+ 125µM 5-FU	+ miR301 mimic	4th	CCL227+ 125µM 5-FU	+ miR301 mimic
5th		+ miR375 mimic	5th		+ miR375 mimic
6th		+ neg. control siRNA	6th		+ neg. control siRNA

3 x 10^6 cells/75 cm^2 flask	5.6 mL/flask
miRNA mimic + HiPerFect®	400 µL/flask
final volume	6 ml/flask

Procedure

The transfection of colorectal cancer cells with microRNA mimics was performed with the HiPerFect® transfection reagent. First, microRNA mimic stock solutions and the negative control siRNA were diluted with RPMI media to a concentration of 30 nM (9 µL mimic miRNA or negative control + 191 µL RPMI). The HiPerFect® stock solution was also diluted in a 1:5 ratio (40 µL HiPerFect® + 160 µL RPMI). Next, cell suspensions of 3 x 10^6 cells in a volume of 5.6 mL RPMI for each transfection were prepared by determination of the cell count/mL with Bürker – Türk counting chambers and dilution. Then 200 µL miRNA mimic solution was incubated for 10 min with 200 µL diluted HiPerFect® transfection reagent for complex formation. The HiPerFect® - mimic miRNA complexes were then pipetted into the 75 cm^2 flasks and distributed by swivelling. Cell suspension were then added slowly to the transfection complexes and incubated for 24 h at 37 °C and 5% CO_2. The next day the transfected cells were lysed and analysed for activation of enzymes of the NF-κB pathway by Western blot (described in chapter 2.4). Furthermore, transcription levels of miRNA in the transfected cells were determined by qPCR (see chapter 2.6).

2.6 microRNA analysis

Quantifying specific miRNAs of interest in colorectal cancer cells was performed by isolating the intracellular RNA followed by cDNA synthesis and quantitative real time PCR. This set of experiments was also conducted with transfected cells to assess if transfections were efficient and how the intracellular content was changed when being transfected.

2.6.1 Lysis of cells and extracellular vesicles

Materials

- TRI Reagent® (Sigma Aldrich)

Procedure

Cell lysis for RNA isolation was done by TRI reagent treatment. Cells were cultivated in T75 flasks to a confluence of 80% and their supernatant was harvested for isolation of extracellular vesicles (described in chapter 2.2.1). The adherent cell monolayer was then washed twice with DPBS and incubated for 5 minutes with 5 mL TRI reagent. Finally, cells were harvested with a cell scraper and 2 mL were used for further RNA isolation. The rest was stored at -80°C.

Isolated extracellular vesicles from the supernatant were resuspended in 400 µL TRI reagent and used for RNA isolation.

2.6.2 RNA isolation

RNA was isolated from cells or extracellular vesicles after treatment thereof with TRI reagent, which is a solution consisting of guanidinium isothiocyanate and phenol, that denatures proteins and solubilizes biological material. Under acidic conditions the addition of chloroform causes a separation of three phases. The upper aqueous phase contains the dissolved RNA, the intermediate phase DNA and the lower organic phase contains proteins. RNA can be isolated further by precipitation from the aqueous phase with isopropanol. (Rio et al., 2010)

Materials

- Chloroform (Sigma Aldrich)
- Isopropanol (Sigma Aldrich)
- Ethanol 75% (Sigma Aldrich)
- H_2O_{DEPC}
- 3 M Na-Acetate (pH=5.5)

Procedure

For RNA isolation, first 0.4 mL chloroform were added to 2 mL lysed cells and 0.1 mL to 0.4 mL lysed extracellular vesicles. Following 15 seconds of vortexing and 15 minutes of incubation at room temperature, the samples were centrifuged at 12000 x g for 15 minutes at 4°C. From this step on the samples were always kept on ice unless indicated otherwise. After centrifugation 3 phases could be observed. The upper, colourless phase containing the RNA was transferred to a new tube containing the same volume of chloroform. After inverting the tubes for 5 minutes, the samples were centrifuged again at 12000 g for 15 minutes at 4°C. For precipitation of the RNA, the aqueous upper phase was transferred again to a new tube and 1 mL of isopropanol were added to cellular samples and 200 µL to extracellular vesicles samples. After mixing the samples by pipetting and incubation of 10 minutes at room temperature, another centrifugation step at 12000 g for 15 minutes at 4°C followed.

Extracellular vesicles RNA pellets were washed with 200 µL ethanol (75%) by slowly and carefully pipetting up and down. Then pellets were first air dried and finally dried at 37°C for 10 minutes. Pellets were resuspended in 9 µl H_2O_{DEPC}. The whole volume was used directly for cDNA synthesis.

Cellular RNA pellets were washed with 2 mL ethanol (75%), vortexed vigorously and centrifuged at 12000 g for 10 minutes at 4°C. After discarding the supernatant consisting of ethanol, the pellets were air-dried at 37°C for 10 minutes. The pellets were dissolved in 50 µL H_2O_{DEPC}, when all the ethanol had evaporated. Afterwards samples were treated overnight with 150 µL Na-acetate solution to obtain a higher concentration and purer RNA. After a centrifugation step at 14000 rpm for 30 minutes at 4°C, the supernatant was discarded. Pellets were washed with 70% ethanol and air-dried first for 5 minutes at room temperature and then for 5 minutes at 37°C. The samples were resuspended in an adequate volume of H_2O_{DEPC}.

The concentration of cellular RNA samples was determined by measurement at 260 nm with Nano Drop® 1000 Spectrophotometer (Thermo Fisher Scientific). The purity of isolated RNA was indicated by $OD_{260/280}$ ratio and $OD_{260/230}$. An absorption of E = 1 at 260 nm corresponds to a ssRNA concentration of 40 µg/mL. Therefore, the concentration of isolated RNA was calculated as shown in Equation 2. H_2O_{DEPC} was used as blank.

$$\boldsymbol{RNA}\left[\frac{\mu g}{mL}\right] = \boldsymbol{OD600} * \mathbf{40}\ \frac{\mu g}{mL} * \boldsymbol{dilution\ factor} \qquad \text{Equation 2}$$

2.6.3 cDNA synthesis

Complementary DNA is generated by reverse transcription of RNA samples with the miScript II RT Kit (Qiagen). The reverse transcriptase mix consists of a combination of poly(A) polymerase for polyadenylation of miRNAs and reverse transcriptase for cDNA synthesis with oligo-dT primers. (Qiagen, 2012)

2.6.3.1 cDNA synthesis of cellular RNA

Materials miScript II RT Kit (50) (Qiagen) Cat. No. 218161:

- 5x miScript HiFlex
- 10x miScript Nucleics Mix
- RNase free water
- miScript Reverse Transcriptase Mix

Procedure

RNA samples were diluted to a concentration of 10 ng RNA in 5 µL RNase-free water (=2 ng/µL). Then cDNA master mixes were prepared as shown in Table 10. The negative control consisted of 5 µL RNase free water + 10 µL master mix. RNA samples are mixed with the master mix in 0.5 mL soft-tubes and cDNA synthesis was performed with the thermocycler PX2 for 60 minutes at 37°C and 5 minutes at 95°C. cDNA was either used for qPCR directly or stored at -20°C.

Table 10: Reagents for cDNA synthesis of cellular RNA

	CONCENTRATION	µL / SAMPLE
miScript HiFlex Buffer	5x	3
miScript Nucleics Mix	10x	1.5
RNase free water	-	4
miScript Reverse Transcriptase Mix	-	1.5
total volume of master mix		10
+ RNA sample	2 ng/µL	5
final volume		15

2.6.3.2 cDNA synthesis of RNA from extracellular vesicles

Materials miScript II RT Kit (50) (Qiagen) Cat. No. 218161:

- 5x miScript HiFlex
- 10x miScript Nucleics Mix
- RNase free water
- miScript Reverse Transcriptase Mix

Procedure

For cDNA synthesis of RNA isolated from extracellular vesicles the whole RNA sample was used directly. The master mixes were prepared as shown in Table 11, mixed with RNA samples and processed also in the thermocycler PX2 for 60 minutes at 37°C and 5 minutes at 95°C. The cDNA was either used for qPCR directly or stored at -20°C. The negative control consisted of 9 µL RNase free water + 6 µL master mix.

Table 11: Reagents for cDNA synthesis of RNA isolated from extracellular vesicles

	CONCENTRATION	µL / SAMPLE
miScript HiFlex Buffer	5x	3
miScript Nucleics Mix	10x	1.5
miScript Reverse Transcriptase Mix	-	1.5
total volume of master mix		6
+ RNA sample	unknown	9
final volume		15

2.6.4 Quantitative Real Time PCR for miRNA

Quantitative real time PCR was performed with the miScript SYBR Green PCR Kit for specific detection of mature microRNAs and quantification thereof. A miRNA specific forward primer and the miScript Universal reverse Primer are used for the polymerase chain reaction, which is detected by SYBR green fluorescence. The relative amount of miRNAs in the samples can be obtained when related to a reference. (Qiagen, 2012)

Materials miScript SYBR Green PCR Kit (200) (Qiagen) Cat. No. 218073

- QuantiTect SYBR Green PCR Master Mix
- miScript Universal Primer
- miScript Primer Assay for the different miRNAs
- RNase-free water

Procedure

Cellular cDNA samples were diluted for qPCR 1:100 (1 µL cDNA + 99 µL RNase free water), whereas cDNA from extracellular vesicles was only diluted 1:2. The reactions were prepared as shown in Table 12 according to Qiagen´s instructions. Small nucleolar RNA RNU48 (Hs_SNORD48_11) served as control for each sample. Quantitative PCR was performed as shown in Table 14 with the Rotor Gene Q (Qiagen) using a 72-well rotor.

Table 12: Reagents for qPCR with cellular cDNA

	CONCENTRATION	µL / SAMPLE
QuantiTect SYBR Green PCR Master Mix	2x	5
miScript Universal Primer	10x	1
miScript Primer Assay	10x	1
RNase free water		1.67
total volume of master mix		8.67
+ cDNA sample (1:100)	unknown	1.33
final volume		10

Table 13: miScript primer assay

PRIMER	TARGET	MIRNA TARGET SEQUENCE
Hs_miR-125b_1	hsa-miR-125b-5p	UCCCUGAGACCCUAACUUGUGA
Hs_miR-141_1	hsa-miR-141-3p	UAACACUGUCUGGUAAAGAUGG
Hs_miR-200c_1	hsa-miR-200c-3p	UAAUACUGCCGGGUAAUGAUGGA
Hs_miR-301a_1	hsa-miR-301a-3p	CAGUGCAAUAGUAUUGUCAAAGC
Hs_miR-375_2	hsa-miR-375	UUUGUUCGUUCGGCUCGCGUGA
Hs_miR-429_1	hsa-miR-429	UAAUACUGUCUGGUAAAACCGU
RNU48 (SNORD48)	NR_002745	-

Table 14: qPCR program

	TEMPERATURE [°C]	TIME
Hold	95	15 min
Cycling (40 cycles)	95	15 sec
	55	30 sec
	70	30 sec

Data analysis

Data from qPCR was analysed by means of the $2^{-\Delta\Delta CT}$ method for relative gene expression analysis (Livak and Schmittgen, 2001). The real efficiency was used for calculations, not the theoretical amplification of 2. RNU48 served as the reference in all samples, since it is stably expressed in cells and extracellular vesicles. The miRNA expression was calculated against the snRNA RNU48 reference using the mathematical model for relative quantification in real-time qPCR according to (Pfaffl, 2001).

$$Ratio = \frac{(E_{target})^{\Delta Ct}target^{(control-sample)}}{(E_{ref})^{\Delta Ct}ref^{(control-sample)}} \qquad \text{Equation 3}$$

3 Results

3.1 Transfer of chemoresistance

The transfer of chemoresistance against 5-fluorouracil (5-FU) via extracellular vesicles from resistant colorectal cancer cells to naïve colorectal cancer cells or to cells with a lower degree of resistance was determined by incubation of naïve or low resistant cell lines with extracellular vesicles isolated from 5-FU chemoresistant cell lines. After incubation over a period of 72 to 168 hours, MTT assays were performed to determine the cytotoxicity of 5-FU. If resistance against 5-FU could be transferred by extracellular vesicles, a shift in the EC_{50} in comparison to the EC_{50} of cell lines not incubated with EVs would be observed.

3.1.1 Transfer of resistance to primary adenoma carcinoma cell line CCL 228

The primary adenoma carcinoma cell line CCL 228 was tested for gaining resistance from extracellular vesicles (EV) isolated from the three resistant cell lines CCL 227 + 5 µM 5-FU, CCL 227 + 25 µM 5-FU and CCL 227 + 125 µM 5-FU. First, a MTT cytotoxicity assay was performed to determine the ideal time for the addition of EVs to the cells. Therefore, three time points were tested: addition of EVs at the beginning of the assay (0 hours), after one day (24 hours) and after four days (96 hours). The resulting EC_{50} values of these three cytotoxicity assays performed in technical triplicates are shown in Figure 6. While only slight variations in the EC_{50} were observed at the first two points in time, a large decrease in EC_{50} could be observed if EVs were added only after four days. Taking these results and the results from the cell line CCL 227 into account (shown below in Figure 9), it was decided to perform further cytotoxicity assays by adding EVs after 24 hours. For each experiment, CCL 228 cells not incubated with EVs served as reference.

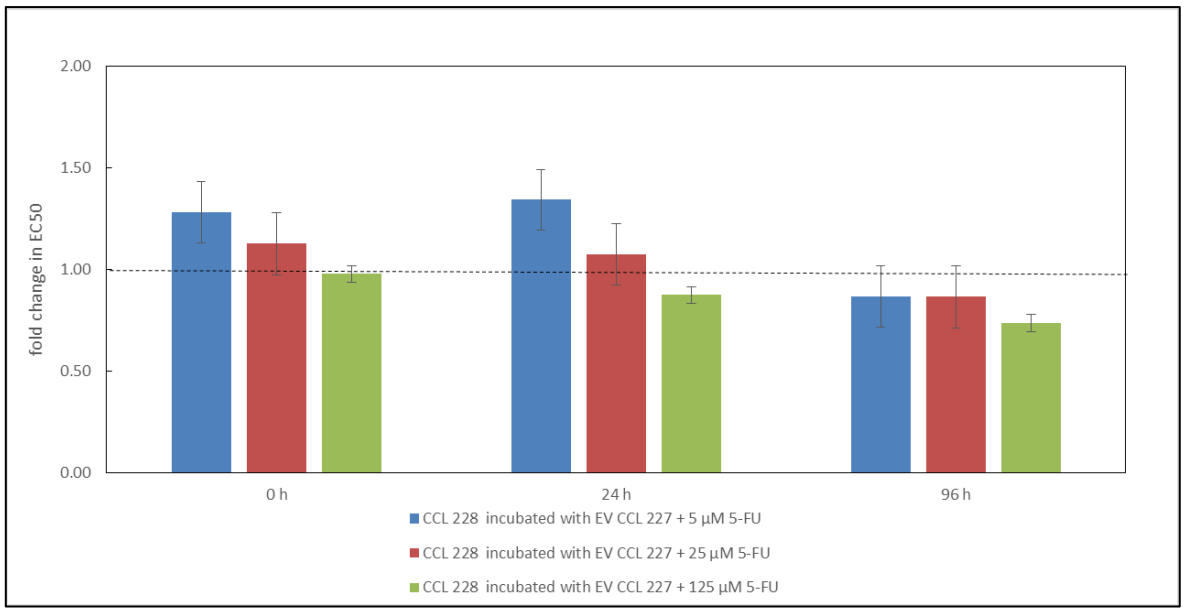

Figure 6: Fold change in EC_{50} of cells incubated with EVs isolated from CCL 227 + 5 µM 5-FU, CCL 227 + 25 µM 5-FU and CCL 227 + 125 µM 5-FU in relation to the EC_{50} of CCL 228. Error bars represent standard error (SE) of technical triplicates.

After establishing the ideal time line for the addition of EVs, further MTT assays with varying conditions were performed to determine the impact on the EC_{50}. Therefore, cells were incubated with different amounts of EVs ranging from 1 µg EVs per 5000 cells to a maximum of 50 µg per 5000 cells. It should be mentioned, that the amount of EVs was determined by Bradford Protein Assay, which is not specific for EVs but determines the whole protein content of the sample and therefore gives only an approximate amount of EVs. MTT Assays were performed for each condition in technical triplicates and the EC_{50} value of the different conditions was determined from sigmoidal dose-response curves, one of which is shown in Figure 7. This data was summarized by calculating the changes in EC_{50} of CCL 228 cells incubated with varying amount of EVs in relation to EC_{50} of CCL 228 cells not incubated with EVs, shown in Figure 8. The addition of high amounts and the addition of low amounts seems to have a lowering effect on the EC_{50}. However, these differences between EC_{50} values were not statistically significant (analysed with GraphPad Prism) and because of a high variability in the results, no further experiments were performed with the cell line CCL 228.

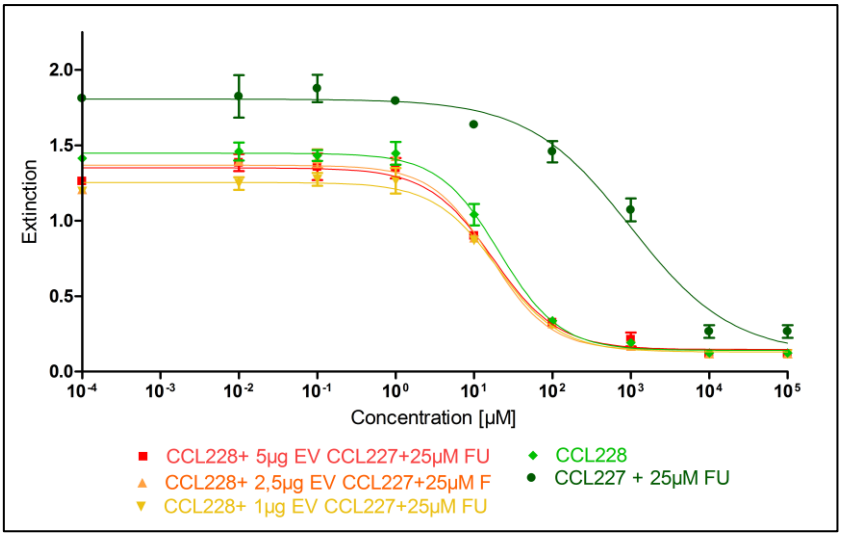

Figure 7: Dose response curve of CCL 228 cells incubated with varying amounts of EVs isolated from CCL 227 + 25 µM 5-FU used to determine EC_{50} values. CCL228 and CCL 227 + 25 µM 5-FU cells incubated with unconditioned media served as controls.

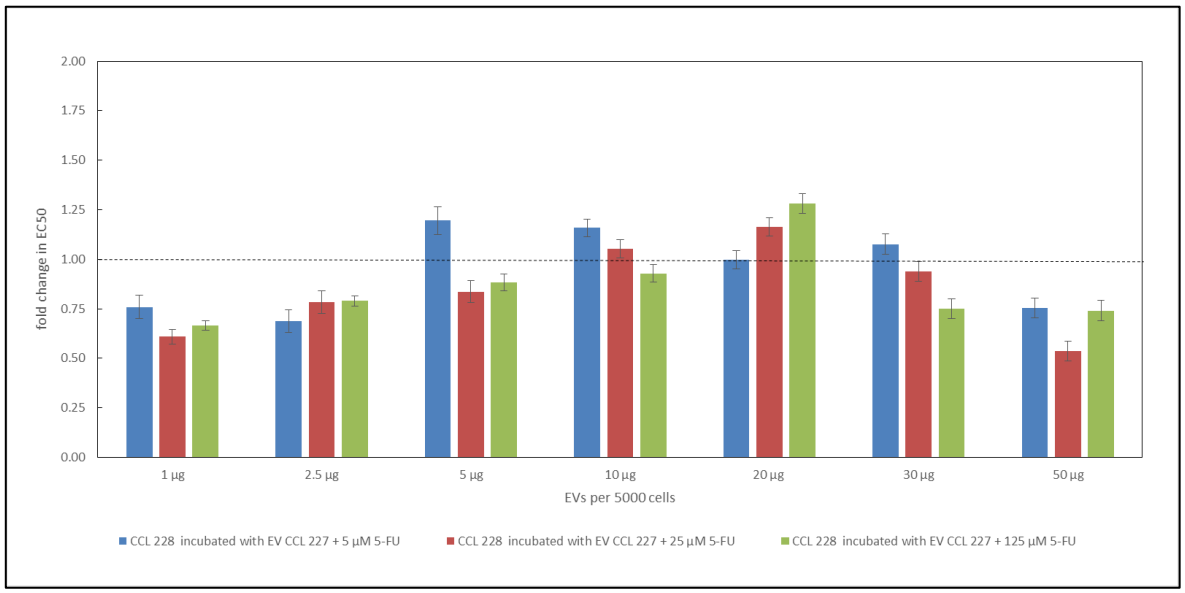

Figure 8: Fold change in EC_{50} determined by MTT assays with varying amounts of EVs added to the cells in relation to the EC_{50} of CCL 228 cells. Error bars represent SE of technical triplicates.

3.1.2 Transfer of resistance to lymph node metastasis cell line CCL 227

The ideal time line for the addition of EVs was also determined for the colorectal cancer cell line CCL 227 by adding EVs at three different points in time during the cytotoxicity assay. First, EVs were added at the beginning of the assay (0h), then after 24 hours and finally after 4 days (96 h). For each experiment, CCL 227 cells not incubated with EVs served as reference. The results (shown in Figure 9) demonstrated, that adding the EVs after 24 hours led to the most evident increase in EC_{50}. Since the main focus was to study increased EC_{50} values, suggesting a transfer of resistance, further cytotoxicity experiments were performed by adding the EVs after 24 hours. Apart from that, the results showed that the addition of EVs after 4 days led to a considerable decrease in EC_{50} values, when the cells were incubated with EVs isolated from the medium or high resistant cell lines.

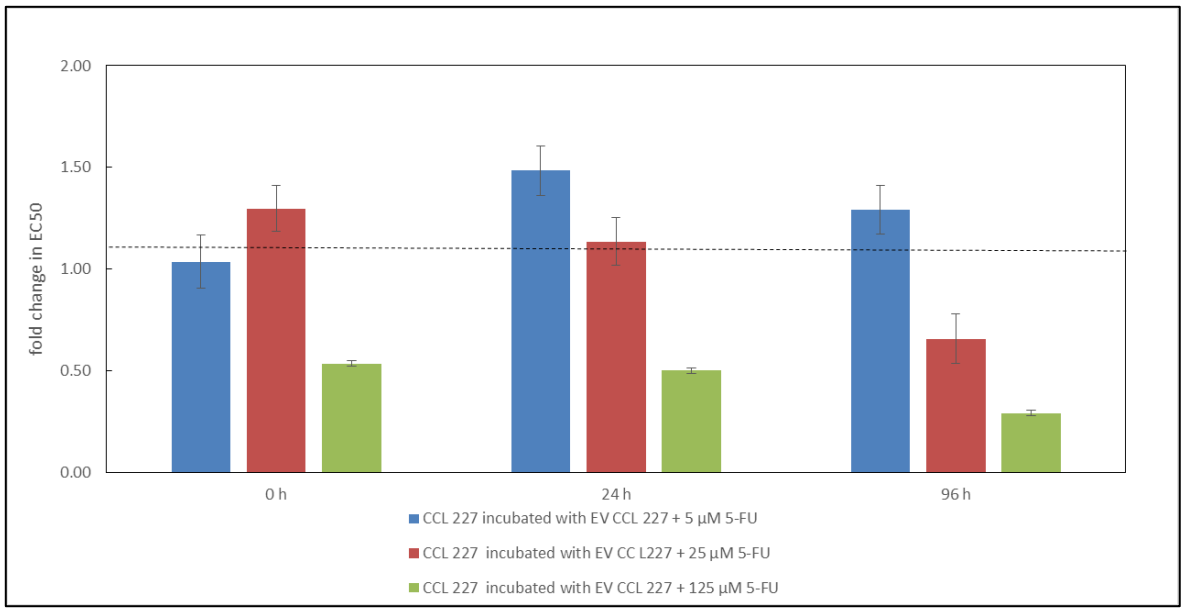

Figure 9: Fold change of EC_{50} of cells incubated for various time periods with EVs isolated from CCL 227 + 5 µM 5-FU, CCL 227 + 25 µM 5-FU and CCL 227 + 125 µM 5-FU in relation to the EC_{50} of CCL 227 cells. Error bars represent SE of technical triplicates.

Afterwards a number of cytotoxicity assays with varying amounts of EVs added to the colorectal cancer cells CCL 227 were performed. By isolating EVs from very large amounts of conditioned media, we were able to incubate the cells with up to 80 µg EVs per 5000 cells. It should be also mentioned here, that the amount of EVs was determined by Bradford Protein Assay, which is not specific for EVs but determines the whole protein content of the sample and therefore gives only an approximate amount of EVs. MTT Assays were performed for each condition and the EC_{50} value of the different conditions was determined from sigmoidal

dose-response curves, one of which is shown in Figure 10. Unfortunately, the results summarized in Figure 11 did variegate widely throughout the different experiments and no direct correlation between the amount of EVs added and the change in EC_{50} could be observed. This variation was also confirmed by numerous repetitions of experiments where initially significant changes in the EC_{50} (analysed with GraphPad Prism) were observed but could not be replicated.

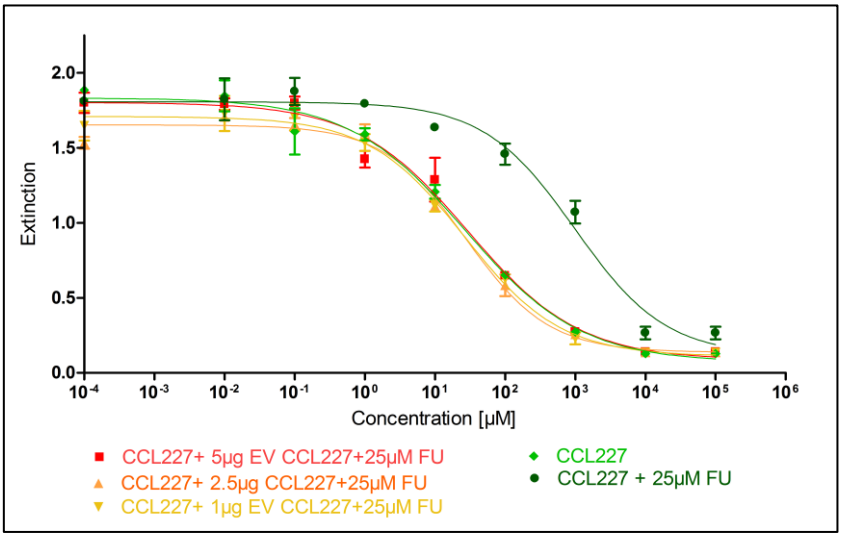

Figure 10: Dose response curve of CCL 227 cells incubated with varying amounts of EVs isolated from CCL 227 + 25 µM 5-FU used to determine EC50 values. CCL228 and CCL 227 + 25 µM 5-FU cells incubated with unconditioned media served as controls.

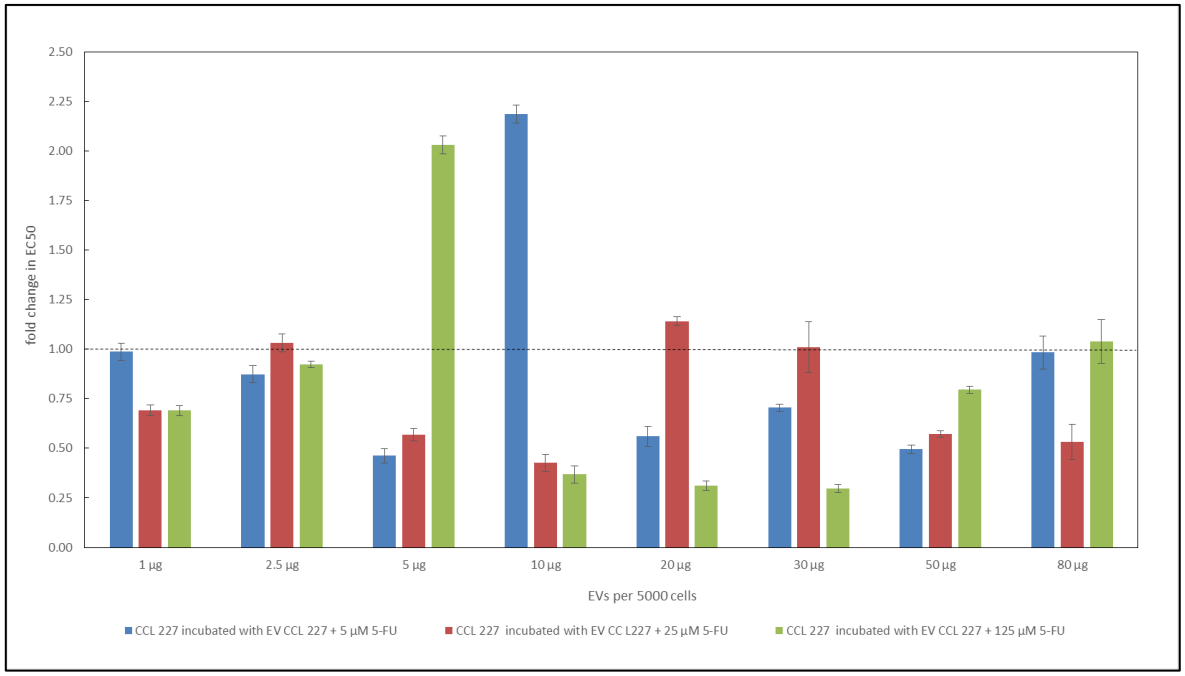

Figure 11: Fold change in EC_{50} determined by MTT assays with varying amounts of EVs added to the cells in relation to the EC_{50} of CCL 227 cells. Error bars represent SE of technical triplicates.

To get a better understanding, why the results fluctuated that heavily, we took a closer look at the experiment conditions. At first, we compared experiments performed with EVs isolated by PEG 6000 precipitation with experiments with EV isolated by differential centrifugation (DC). As shown in Figure 12, results from assays performed with PEG isolated EVs fluctuated overall much more than those from assays performed with DC isolated EVs showing average coefficients of variations of ± 53% and ± 35% respectively. This suggests, that by using DC isolated EVs in further experiments, variations within the results could be minimised to some extent. Furthermore, EVs isolated by PEG seem to have on the average no effect on the fold change of EC_{50}, whereas EVs isolated by differential centrifugation show a clearly negative effect on the EC_{50} when isolated from the cell lines CCL 227 + 5 µM 5-FU and CCL 227 + 25 µM 5-FU and a positive effect by increasing the EC_{50} when isolated from the high resistant cell line CCL 227 + 125 µM 5-FU. It should be mentioned, that only three experiments were performed with EVs isolated by differential centrifugation and ten experiments with PEG precipitated EVs.

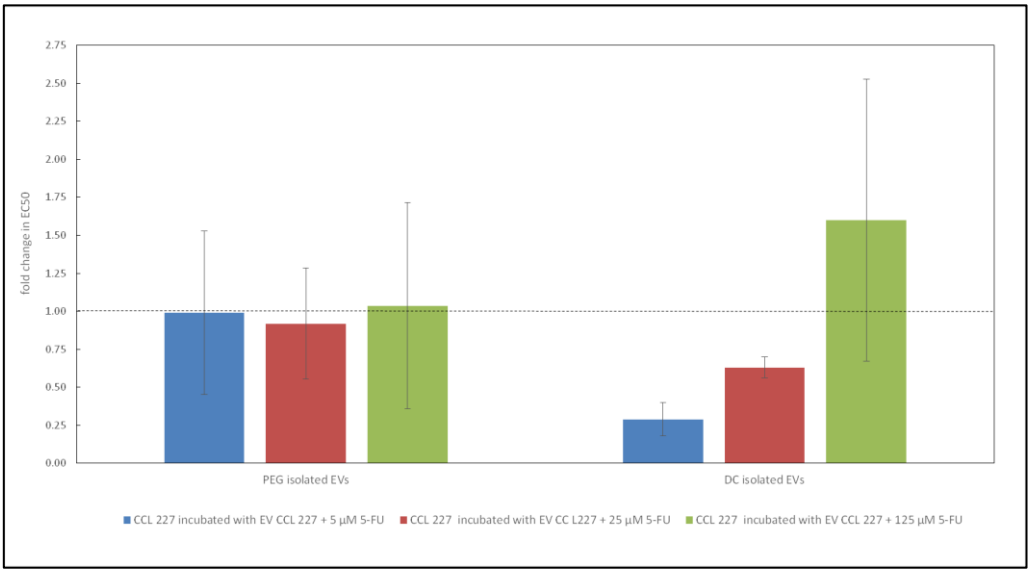

Figure 12: Average EC_{50} fold change ± standard deviation (SD) of biological replicates in cytotoxicity experiments performed with either EVs isolated by PEG 6000 precipitation or by differential centrifugation

Another condition which varied throughout the experiments, was whether EVs were used directly after isolation or stored intermediately at -80°C. As shown in Figure 13 results from assays performed with EVs stored at -80°C fluctuated more than those from assays performed with fresh EVs showing average coefficients of variations of ± 53% and ± 46% respectively. Even though there is only a rather small difference in the variations between this two conditions, fresh isolated EVs directly used for experiments should be favoured in further experiments. Furthermore, EVs could have been damaged to some extend by storage at -80°C, since they were resuspended in PBS (1x) without any addition of cryoprotectant agents.

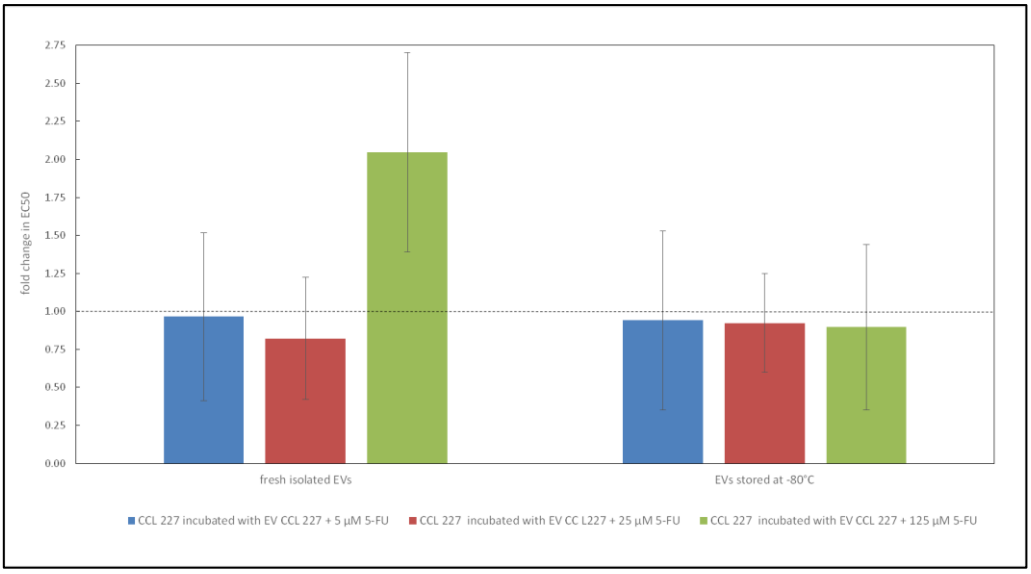

Figure 13: Average EC_{50} fold change ± SD of biological replicates in cytotoxicity experiments performed with either freshly isolated EVs or with EVs stored at -80°C

Since the cell line CCL 227 showed the most promising results, it was chosen for all further experiments (PDT assays, NF-κB kinetic and transfections). However, it should be taken into consideration that EV isolation and especially EV characterisation as well as proper quantification should be optimised.

3.1.3 Transfer of resistance to primary colorectal carcinoma cell lines CaCo2 and CCL 247

Parallel to testing the transfer of resistance by extracellular vesicles in the cell line CCL 227, this was also studied in the cell lines CaCo2 and CCL 247, which are more sensitive to 5-fluorouracil than CCL 228 and CCL 227. These experiments were performed under non optimized conditions with PEG isolated EVs partially stored at -80°C. The incubation of CCL 247 cells with EVs from chemoresistant cell lines showed no impact on the EC_{50} (shown in Table 15).

Table 15: Average EC_{50} fold change ± SD of biological replicates determined by MTT assays after incubation of cells with EVs from resistant cell lines against CCL 247 not incubated with EVs

CCL 247 CELLS INCUBATED WITH	AVERAGE EC_{50} FOLD CHANGE
EVs isolated from CCL 227	0.73
EVs isolated from CCL 227 + 5 µM 5-FU	1.17 ± 0.18
EVs isolated from CCL 227 + 25 µM 5-FU	0.89 ± 0.38
EVs isolated from CCL 227 + 125 µM 5-FU	0.76 ± 0.20

The incubation of CaCo2 cells with EVs from the low and intermediate resistant cell lines showed an increased EC_{50}, but no effect when incubated with EVs from the high resistant cell line (Table 16). Also, in these experiments the results varied widely with an average coefficient of variation of ± 42%, probably again due to experimental conditions and lacking robustness of the method.

Table 16: Average EC_{50} fold change ± SD of biological replicates determined by MTT assays after incubation of cells with EVs from resistant cell lines against CaCo2 not incubated with EVs

CaCo2 cells incubated with	Average EC_{50} fold change
EVs isolated from CCL 227	1.06 ± 0.12
EVs isolated from CCL 227 + 5 µM 5-FU	1.38 ± 0.59
EVs isolated from CCL 227 + 25 µM 5-FU	2.29 ± 1.48
EVs isolated from CCL 227 + 125 µM 5-FU	0.98 ± 0.49

3.1.4 Transfer of resistance between chemoresistant cell lines

Simultaneously to the experiments previously mentioned, transfer of resistance between resistant cell resistant cell lines was tested by incubation of the low and intermediate resistant cell line with EVs EVs isolated from respectively higher resistant cell lines. These experiments were performed under under non optimized conditions with PEG isolated EVs partially stored at -80°C. No clear effect on the on the resistance level of CCL 227 + 5 µM 5-FU was seen when incubated with EVs isolated from from CCL 227 + 25 µM 5-FU and CCL 227 + 125 µM 5-FU (data shown in Table 17). On the contrary, a clear reduction was observed when the intermediate resistant cell line was incubated with EVs isolated from the high resistant cell line (data shown in

Table 18).

Table 17: Average EC_{50} fold change ± SD of biological replicates determined by MTT assays after incubation of cells with EVs from the intermediate and high resistant cell lines against CCL 227 + 5 µM 5-FU not incubated with EVs

CCL 227 + 5 µM 5-FU cells incubated with	Average EC_{50} fold change
EVs isolated from CCL 227 + 25 µM 5-FU	1.18 ± 0.11
EVs isolated from CCL 227 + 125 µM 5-FU	0.92 ± 0.51

Table 18: Average EC_{50} fold change ± SD of biological replicates determined by MTT assays after incubation of cells with EVs from high resistant cell lines against CCL 227 + 25 µM 5-FU not incubated with EVs

CCL 227 + 25 µM 5-FU cells incubated with	Average EC_{50} fold change
EVs isolated from CCL 227 + 125 µM 5-FU	0.66 ± 0.02

3.2 PDT Assay

The impact of extracellular vesicles (EV) on the growth of naïve cell line CCL 227 was further studied with PDT assays. The determination of their population doubling time (PDT) after exposure to EV isolated from cell lines with progressing stages of resistance should give deeper insight on the effects on growth and cell viability. Therefore, CCL 227 cells were incubated with EVs isolated from CCL 227 + 5 µM 5-FU, CCL 227 + 25 µM 5-FU and CCL 227 + 125 µM 5-FU over a time period of 7 days (168 hours). Cell viability was measured at 5 points in time (24 h – 48 h – 72 h – 100 h – 168 h) by the addition of MTT salt and detection of viable cells with a spectrophotometer. Results are shown in Table 19. The last time point (168h) was not included in the results, because the cells were already in stationary phase. PEG precipitated medium was used as a negative control.

Table 19: Population doubling times (PDT) calculated by means of the slope of cytotoxicity curves

CCL 227 INCUBATED WITH	PDT
-	25.3
negative control	27.9
EVs isolated from CCL 227 + 5 µM 5-FU	28.9
EVs isolated from CCL 227 + 25 µM 5-FU	31.7
EVs isolated from CCL 227 + 125 µM 5-FU	57.4

The population doubling time is distinctly prolonged 2.3 fold, when cells of the naive cell line CCL 227 were incubated with EVs from the high resistant lymph node metastasis cell line. On the other hand, incubation with EVs from the low and intermediate resistant cell lines had no clear impact. This supports the observed slower growing of cells incubated with EVs from CCL 227 + 125 µM 5-FU in the MTT assays.

3.3 NF-κB signalling pathway kinetics

Since it was previously shown that the NF-κB signalling pathway is activated in chemoresistant lymph node metastasis cell lines (Korber et al., 2016), it was of interest to study whether this activation could be transferred by extracellular vesicles. Therefore, the effects of extracellular vesicles from resistant lymph node metastasis cell lines on the NF-κB pathway of the naïve lymph node metastasis cell line was assessed by incubation, followed by cell lysis, protein extraction and immunoblotting. The naïve CCL 227 cells were incubated with varying amounts of extracellular vesicles and harvested at different time points. Activation of the NF-κB signalling pathway was then analysed by Western blot against IKKα, IKKβ, IκBα, p65 and their phosphorylated forms phospho-IKKα/IKKβ, phospho-IκBα and phospho-p65. The housekeeping GAPDH served as control. If the NF-κB pathway would be activated by incubation with EVs, phosphorylated forms should be present in the cells. Three NF-κB kinetics were performed with CCL 227 cells incubated either with isolated EVs or with PEG precipitated or ultracentrifuged unconditioned medium (neg. control). Furthermore, CCL 227 cells not incubated with EVs or medium were used as reference and CCL 227 + 125 µM 5-FU lysates as positive control. The sample code for all following Western blots is stated in Table 20.

Table 20: Sample code of the NF-κB kinetics for immunoblots

SAMPLE NO.	1ST NF-κB KINETIC	2ND NF-κB KINETIC	3RD NF-κB KINETIC
1	0h CCL 227	0h CL 227 + 125 µM 5-FU	0h CCL 227 + 125 µM 5-FU
2	1h CCL 227 + neg. control	0h CCL 227	0h CCL 227
3	1h CL 227 + 390 µg EVs	1h CCL 227 + neg. control	1h CCL 227 + neg. control
4	4h CCL227 + neg. control	1h CCL 227 + 790 µg EVs	1h CCL 227 + UZ EVs
5	4h CCL 227 + 390 µg EVs	4h CCL 227 + neg. control	4h CCL 227 + neg. control
6	24h CCL 227 + neg. control	4h CCL 227 + 790 µg EVs	4h CCL 227 + UZ EVs
7	24h CCL 227 + 390 µg EVs	24h CCL 227 + neg. control	24h CCL 227 + neg. control
8	--	24h CCL 227 + 790 µg EVs	24h CCL 227 + UZ EVs

The presence of IKKα could not be observed in any of the three NF-κB kinetics, only some unspecific bands at lower molecular weights were detected (data not shown). Activated IKKα was also not detectable in the resistant cell line CCL 227 + 125 µM 5-FU and the naïve cell line CCL 227 incubated with EVs thereof.

The next enzyme in the NF-κB signalling cascade, IKKβ, was present in the naïve cell line CCL 277 regardless whether incubated with extracellular vesicles or not. On the other hand, IKKβ seemed not always to be present or detectable in the high resistant cell line CCL 227 + 125 µM 5-FU (Figure 14). The phosphorylated form of IKKβ was not detectable in neither the resistant cell line nor the naïve cell line incubated with EVs (data not shown).

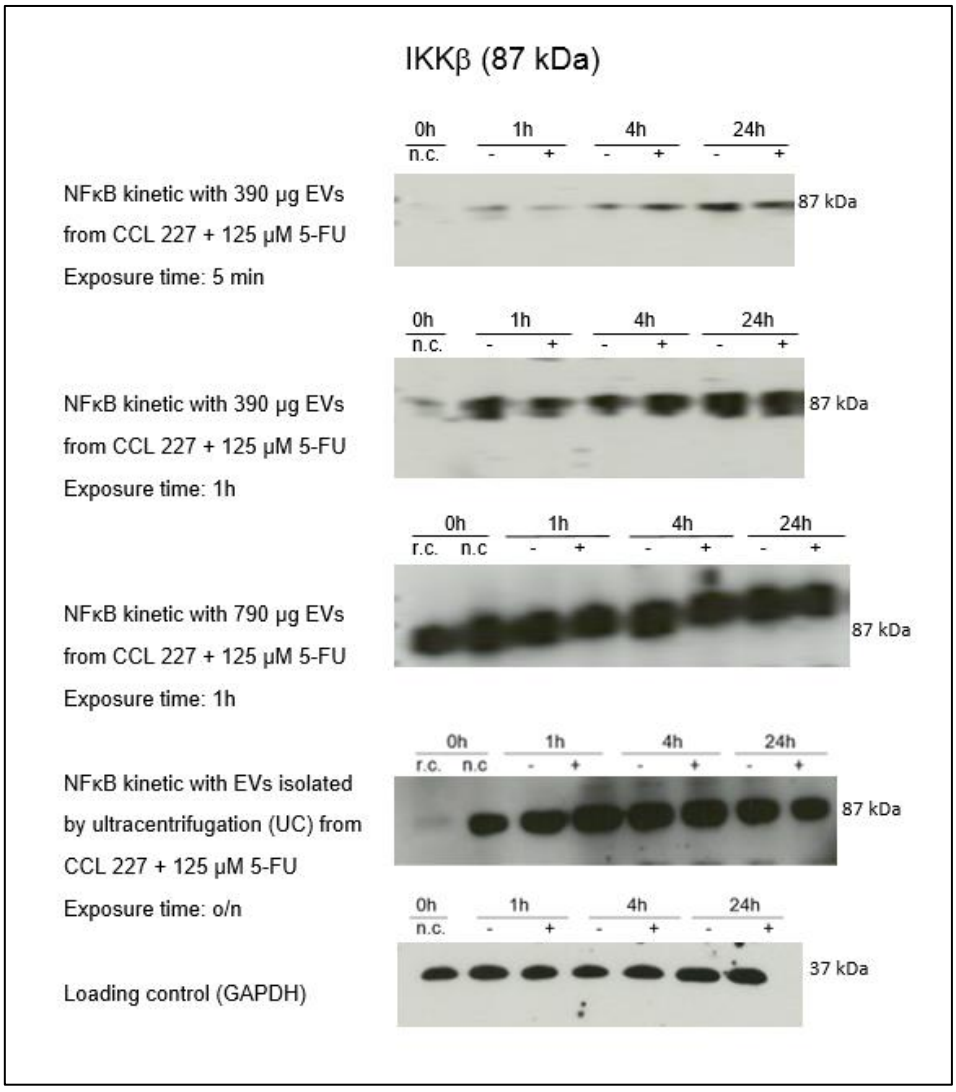

Figure 14: Immunoblot to detect IKKβ in CCL 227 cells incubated with varying amounts of EVs isolated from CCL 227 + 125 µM 5-FU using anti-rabbit secondary antibody. The blots show CCL 227 cells incubated for 1h, 4h or 24h with EVs (indicated as +) or media treated as conditioned media used for EV isolation (indicated as -). CCL 227 cells and CCL 227 + 125 µM 5-FU cells, indicated as n.c. (native cells) and r.c. (resistant cells) respectively, served as controls. GAPDH was used as loading control for each blot.

The presence of the enzyme IκBα in CCL 227 cells seemed not to be influenced by incubation with EVs, since it was also detectable in cells incubated with the negative control. On the other hand, the CCL 227 + 125 µM 5-FU sample showed no or only very light bands, meaning that IκBα is barely present in cell lysates (Figure 15). The phosphorylated form of IκBα proofed to be challenging for Western blot, since the antibody was binding unspecifically to the marker. Furthermore, mainly unspecific bands at lower molecular weights were detected and no distinct presence of phosphorylated IκBα could be observed (data not shown).

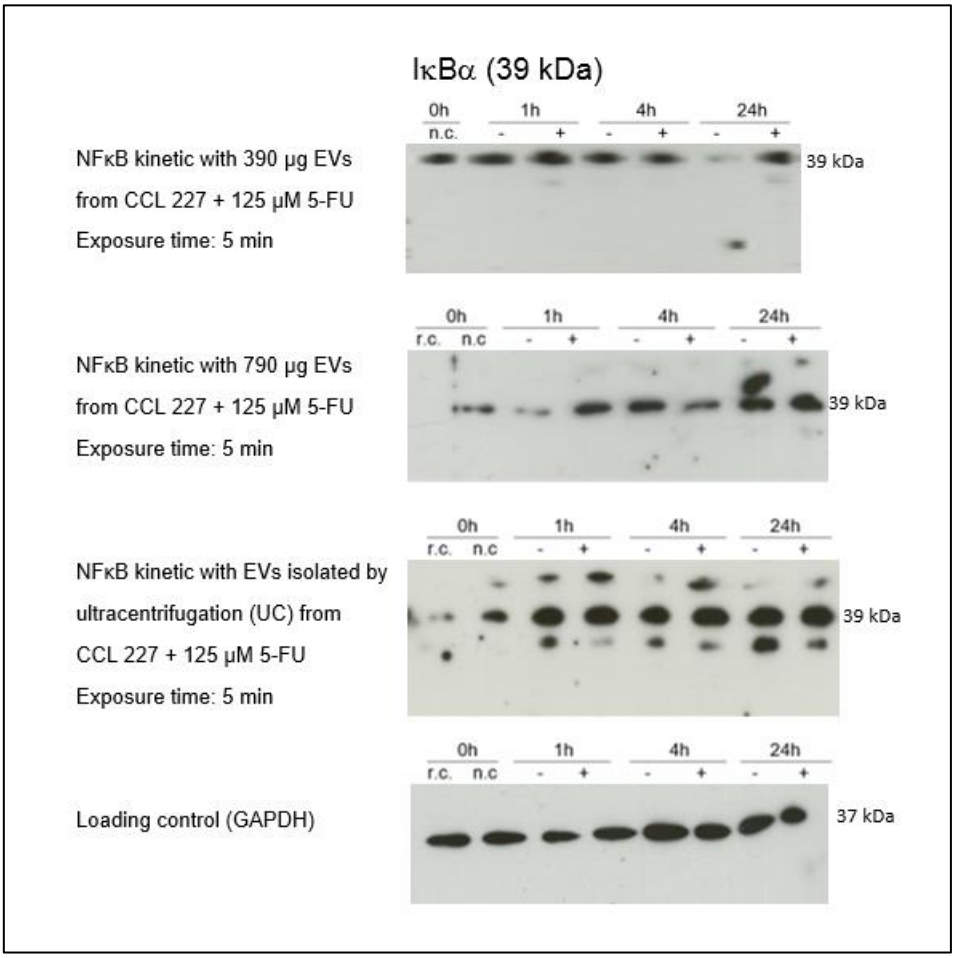

Figure 15: Immunoblot to detect IκBα in CCL 227 cells incubated with varying amounts of EVs isolated from CCL 227 + 125 µM 5-FU using anti-mouse secondary antibody. The blots show CCL 227 cells incubated for 1h, 4h or 24h with EVs (indicated as +) or media treated as conditioned media used for EV isolation (indicated as -). CCL 227 cells and CCL 227 + 125 µM 5-FU cells, indicated as n.c. (native cells) and r.c. (resistant cells) respectively, served as controls. GAPDH was used as loading control for each blot.

Finally, the protein extracts were blotted against the enzyme involved in the last step of the NF-κB signalling pathway p65 and its phosphorylated form phospho-p65. While p65 was detected beautifully in all samples with equally strong bands (Figure 16), its phosphorylated form showed less intense bands (Figure 17). No difference between cells incubated with extracellular vesicles and cells incubated with unconditioned media was observable.

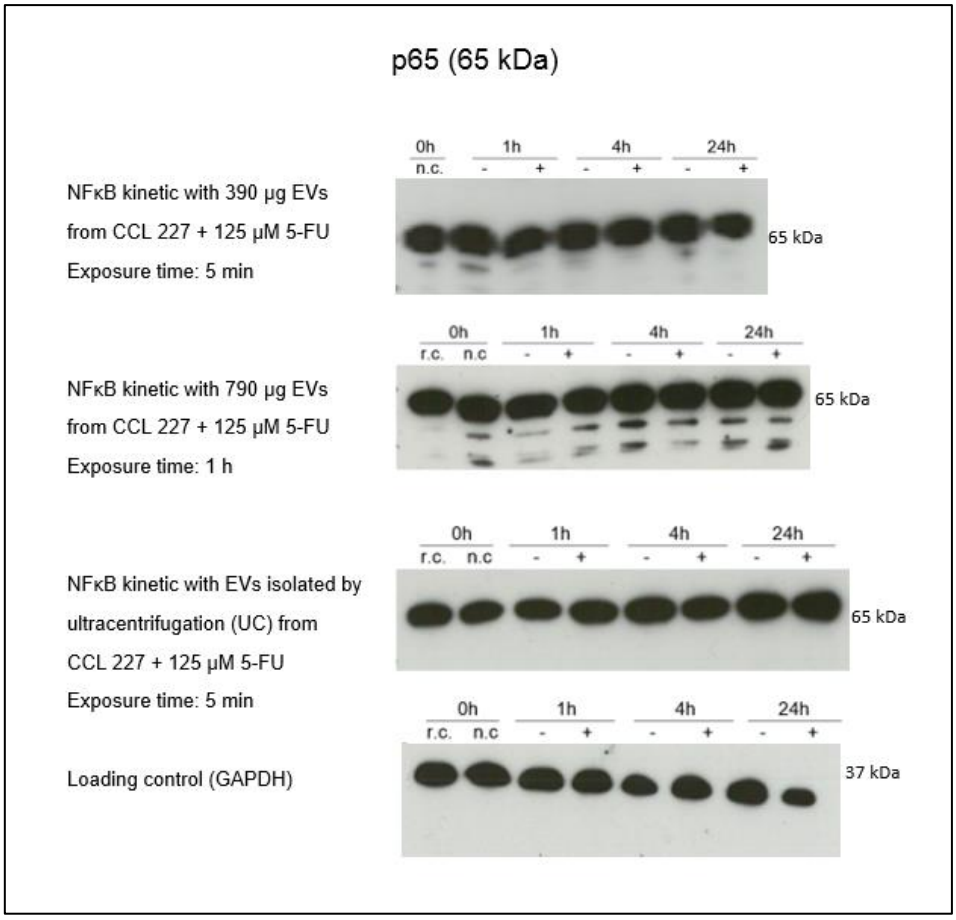

Figure 16: Immunoblot to detect p65 in CCL 227 cells incubated with varying amounts of EVs isolated from CCL 227 + 125 µM 5-FU using anti-rabbit secondary antibody. The blots show CCL 227 cells incubated for 1h, 4h or 24h with EVs (indicated as +) or media treated as conditioned media used for EV isolation (indicated as -). CCL 227 cells and CCL 227 + 125 µM 5-FU cells, indicated as n.c. (native cells) and r.c. (resistant cells) respectively, served as controls. GAPDH was used as loading control for each blot.

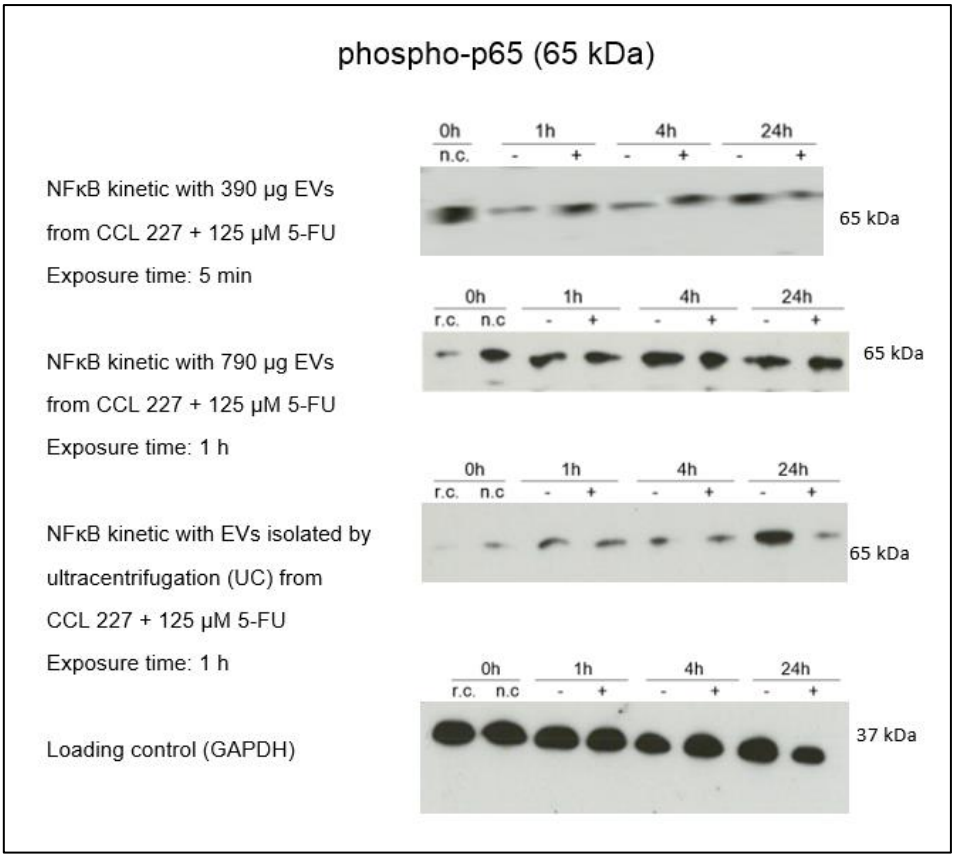

Figure 17: Immunoblot to detect phospho-p65 in CCL 227 cells incubated with varying amounts of EVs isolated from CCL 227 + 125 µM 5-FU using anti-rabbit secondary antibody. The blots show CCL 227 cells incubated for 1h, 4h or 24h with EVs (indicated as +) or media treated as conditioned media used for EV isolation (indicated as -). CCL 227 cells and CCL 227 + 125 µM 5-FU cells, indicated as n.c. (native cells) and r.c. (resistant cells) respectively, served as controls. GAPDH was used as loading control for each blot.

Since there was clearly no correlation to be found between the presence of activated enzymes of the NF-κB pathway and incubation of cells with extracellular vesicles, it is reasonable to assume that the activation cannot be transferred from chemoresistant cell lines to naïve cell lines with extracellular vesicles. Furthermore, we were also not able to show that the NF-κB pathway was activated entirely in the high resistant CCL 227 + 125 µM 5-FU cell line. However, it should be taken into consideration that also in this set of experiments, EV isolation and characterisation as well as proper quantification should be optimised. It would be of great interest to assess the presence of NF-κB signalling enzymes inside the EVs themselves, as well as to determine whether the enzymes are selectively packed into EVs. This could be achieved by comparing the amount of these enzymes inside EVs to the amount of NF-κB enzymes inside the EV releasing cells.

3.4 NF-κB signalling pathway regulation with microRNA

Simultaneously to the evaluation whether the NFkB signalling pathway can be activated by extracellular vesicles from chemoresistant cell lines, the influence of microRNA on activation of this pathway was studied.

3.4.1 Microarray data analysis

Previously obtained Exiqon microarray data from two naïve cell lines CCL 228, CCL 227 and from three resistant cell lines CCL 227 + 5 µM 5-FU, CCL 227 + 25 µM 5-FU and CCL 227 + 125 µM 5-FU was analysed for differentially expressed microRNAs, which according to literature can have an effect on the NF-κB pathway. This was achieved by comparison of microRNA expression levels (G-values) among the different cell lines (Figure 18 and Figure 19). According to this comparison and literature, six microRNAs differentially expressed in colorectal cancer cells were chosen to be further analysed: miR-375-3p, miR-429-5p, miR-200c-3p, miR-301a-3p, miR-125-5p, miR-141-3p.

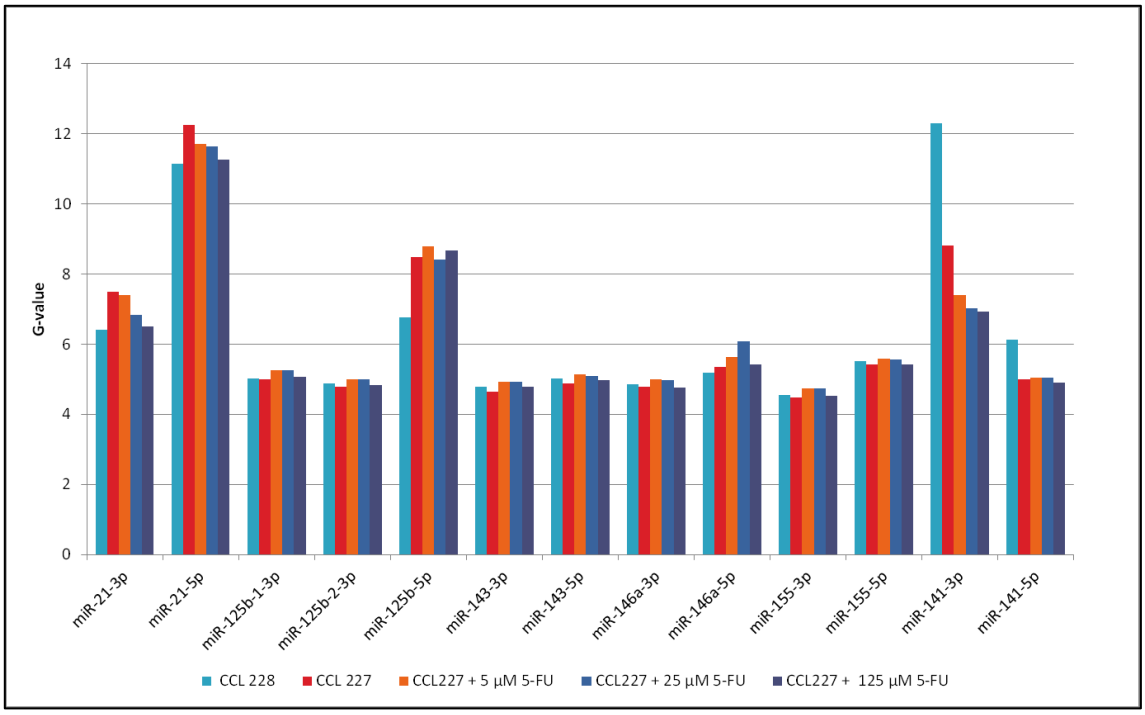

Figure 18: Expression levels of selected miRNA according to microArray data

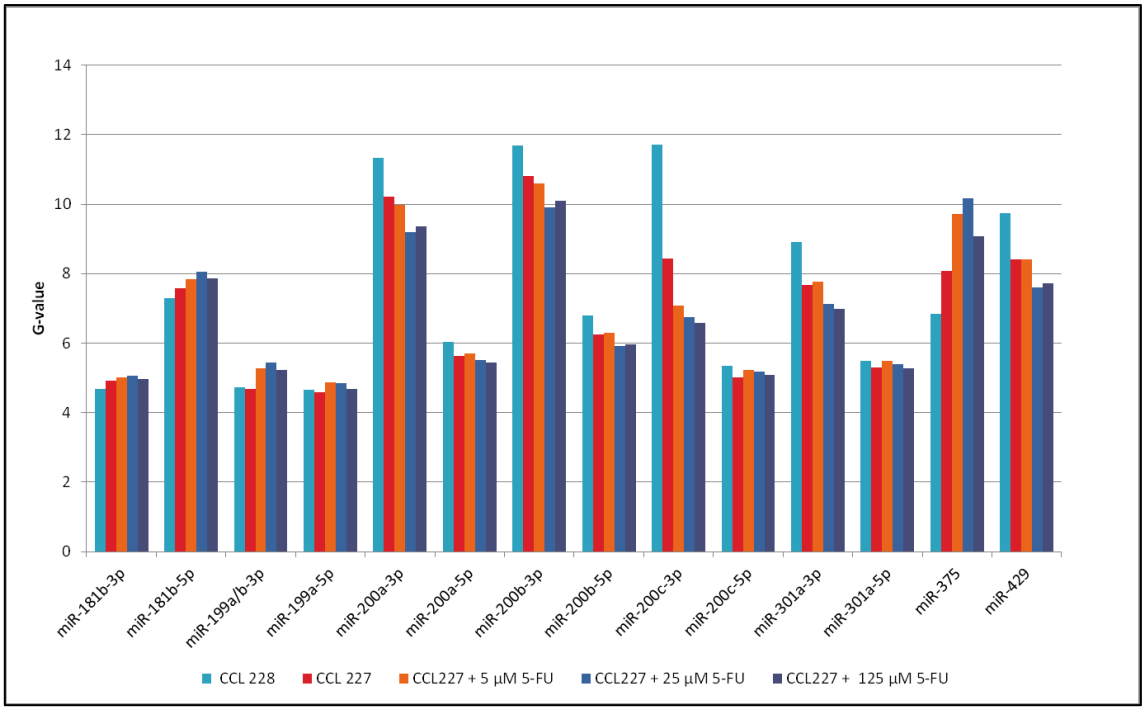

Figure 19: Expression levels of selected miRNA according to microarray data

3.4.2 Validation of microRNA expression

Differential expression of the six selected microRNAs in colorectal cancer cell lines was validated by real-time PCR. The whole RNA content was isolated from cells and from secreted extracellular vesicles and reverse transcribed into cDNA, which was then used for real-time PCR. Expression levels of microRNAs were compared amongst the different cell lines by calculating the fold changes. From all six analysed microRNAs, miR-301a and miR-375-3p showed the highest changes in expression in between colorectal cancer cell lines (Table 21 and Table 22, data of other microRNAs shown in appendix). Furthermore, differences could be observed in cellular and EV expression levels for this two microRNAs. Since we wanted to assess whether microRNAs, which according to literature have an impact on the NF-κB pathway, may be transferred via extracellular vesicles from resistant cell lines to naïve cell lines, a difference between cellular and EV expression was of particular interest. Based on these findings, miR-301a and miR-375-3p were chosen for further analysis.

Table 21: Fold changes in expression levels of miR-301a. The expression in CCL 227, CCL 227 + 5 µM 5-FU, CCL 227 + 25 µM 5-FU CCL 227 + 125 µM 5-FU cells and extracellular vesicles (EVs) was compared to the expression in respectively lower resistant cell lines and their EVs. Fold changes lower than one signify downregulation, whereas fold changes higher than one signify upregulations.

FOLD CHANGE OF ↓ IN COMPARISON TO →	CCL 228		CCL 227		CCL 227 + 5 µM 5-FU		CCL 227 + 25 µM 5-FU	
	CELLS	EVS	CELLS	EVS	CELLS	EVS	CELLS	EVS
CCL 227	0.32	1.66						
CCL 227 + 5 µM 5-FU			2.89	1.26				
CCL 227 + 25 µM 5-FU			4.72	0.76	1.66	0.61		
CCL 227 + 125 µM 5-FU			1.60	0.40			0.34	0.54

Table 22: Fold changes in expression levels of miR-375-3p. The expression in CCL 227, CCL 227 + 5 µM 5-FU, CCL 227 + 25 µM 5-FU CCL 227 + 125 µM 5-FU cells and extracellular vesicles (EVs) was compared to the expression in respectively lower resistant cells and EVs. Fold changes lower than one signify downregulation, whereas fold changes higher than one signify upregulations.

FOLD CHANGE OF ↓ IN COMPARISON TO →	CCL 228		CCL 227		CCL 227 + 5 µM 5-FU		CCL 227 + 25 µM 5-FU	
	CELLS	EVS	CELLS	EVS	CELLS	EVS	CELLS	EVS
CCL 227	2.33	1.79						
CCL 227 + 5 µM 5-FU			3.59	2.39				
CCL 227 + 25 µM 5-FU			5.62	4.30	1.58	1.82		
CCL 227 + 125 µM 5-FU			2.00	1.46			0.38	0.33

3.4.3 Transfection of CCL 227 cells with microRNAs

The influence of the two finally selected microRNAs, miR-301a and miR-375-3p, on the naïve cell line CCL 227 was examined by transfection, followed by studying the impact thereof on the cells. Therefore, CCL 227 cells were transfected for 24 hours with the miRNA mimics miR-301a and miR-375-3p followed by the identification of the transcription levels via real-time PCR. The transfection should also give insight, if this specific microRNAs activate proteins of the NFκB signalling pathway. The 5-FU resistant cell line CCL 227 + 125 µM 5-FU was also transfected with the miRNA mimics miR-301a and miR-375-3p and served as a control.

3.4.3.1 Expression levels of miR-301a and miR-375-3p

Expression levels of miR-301a and miR-375-3p were attained after RNA isolation from transfected cells and their secreted extracellular vesicles (EVs), cDNA synthesis and real-time PCR. The housekeeping snRNA RNU48 served as control and reference for calculations. As shown in Figure 20 and Figure 21, the expression of both miRNAs in the cell line CCL 227, when transfected, was upregulated at the same level inside the cell, as well as in EVs. Furthermore, it was observed that miR-375-3p is downregulated in EV, when CCL227 are transfected with miR301a.

The high resistant cell line CCL 227 + 125 µM 5-FU transfected with miR-301a had a four times higher expression level inside the cells than in the extracellular vesicles (Figure 20). On the other hand, when transfected with miR-375-3p, 9 times more miRNA was found inside EVs (Figure 21). However, it should be mentioned, that RNU48 suffices only partly as control for EVs due to its unspecificity.

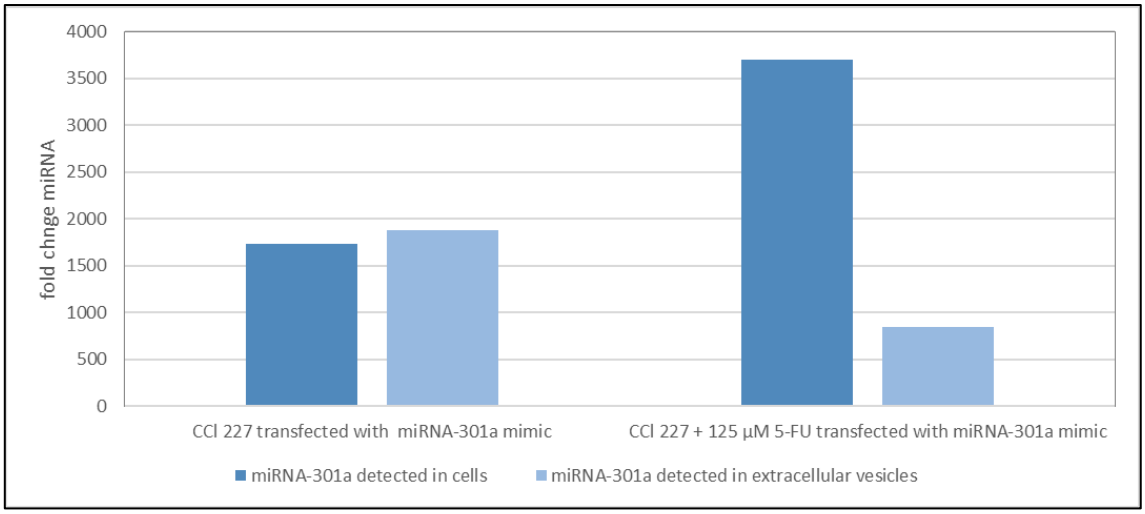

Figure 20: Fold change of miR-301a expression levels in naïve CCL 227 cells and resistant CCL 227 + 125 µM 5-FU cells and their EVs after transfection in relation to snRNA RNU48 control expression levels. Calculated according to Pfaffl (see chapter 2.6.4) from technical quadruplicates.

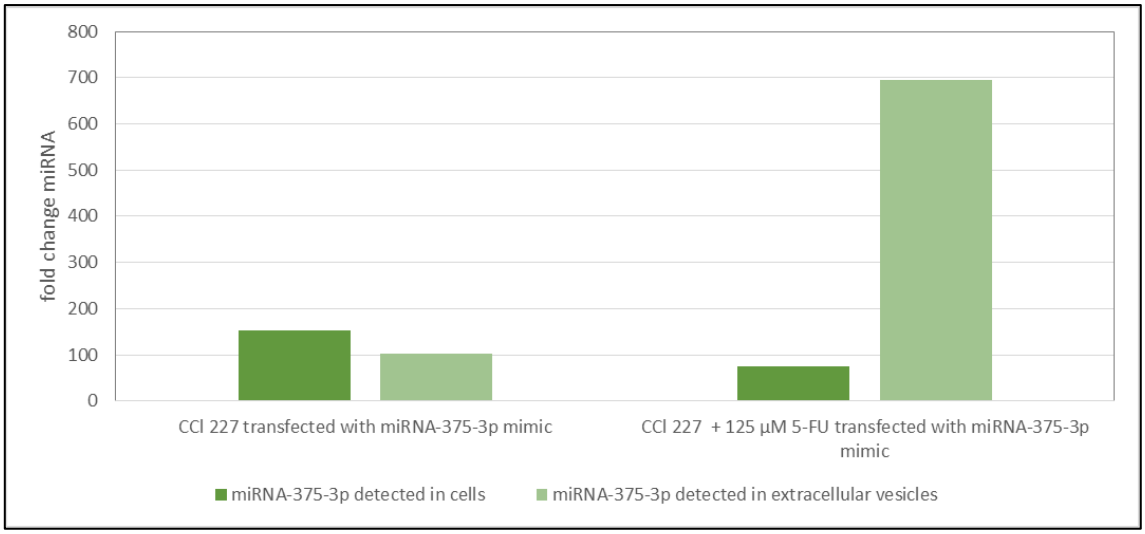

Figure 21: Fold change of miR-375-3p expression levels in naïve CCL 227 cells and resistant CCL 227 + 125 µM 5-FU cells and their EVs after transfection in relation to snRNA RNU48 control expression levels. Calculated according to Pfaffl (see chapter 2.6.4) from technical quadruplicates.

The cells transfected with miR-301a mimic were also analysed for miR-375-3p expression levels and vice versa, to determine any reverse effects. The exact fold changes in expression levels of microRNAs in cells and EVs after transfection in comparison to the housekeeping snRNA RNU48 are shown in Table 23 and Table 24.

Table 23: Fold changes in expression levels of miR-301a in cells and EVs referring to snRNA RNU48 control. Fold changes lower than one signify downregulation, whereas fold changes higher than one signify upregulations.

	CELLS	EVS
CCl 227 transfected with miR-301a mimic	1735.7	1875.3
CCl 227 transfected with miR-375-3p mimic	1.9	2.6
CCl 227 + 125 µM 5-FU transfected with miR-301a mimic	3701.0	847.4
CCl 227 + 125 µM 5-FU transfected with miR-375-3p mimic	11.8	1.9

Table 24: Fold changes in expression levels of miR-375-3p in cells and EVs referring to snRNA RNU48 control. Fold changes lower than one signify downregulation, whereas fold changes higher than one signify upregulations.

	CELLS	EVS
CCl 227 transfected with miR-301a mimic	3.5	0.4
CCl 227 transfected with miR-375-3p mimic	153.0	102.8
CCl 227 + 125 µM 5-FU transfected with miR-301a mimic	0.4	2.5
CCl 227 + 125 µM 5-FU transfected with miR-375-3p mimic	74.0	695.7

3.4.3.2 NF-κB activation after transfection

The activation of the NF-κB signalling pathway in naïve CCL 227 cells and resistant CCL 227 + 125 µM 5-FU after transfection with miR-301a and miR-375-3p was tested by Western blot. The cell lysates were analysed against and their phosphorylated forms phospho-IKKα/IKKβ and phospho-IκBα. The housekeeping GAPDH served as control. Activation of the NF-κB pathway could be observed, if the phosphorylated forms of these three proteins were present in the cells. However, the immunoblots depicted in Figure 22 show no significant activation of the NF-κB pathway after transfection with miR-301a and miR-375-3p.

Table 25: Sample code for immunoblots of cells transfected with miR-301and miR-375-3p mimics

CELL LINE	TRANSFECTED WITH
CCL 227	+ negative control siRNA
	+ 30 nM miR-301a
	+ 30 nM miR-375-3p
CCL 227 + 125 µM 5-FU	+ negative control siRNA
	+ 30 nM miR-301a
	+ 30 nM miR-375-3p

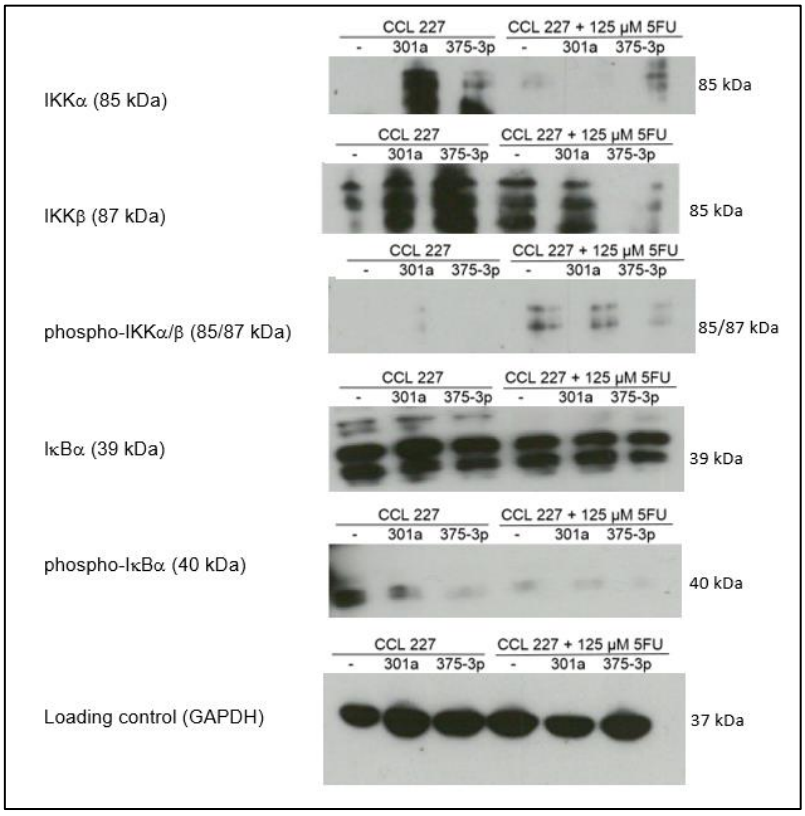

Figure 22: Immunoblots of cellular protein extracts after transfection of CCL 227 and CCL 227 + 125 µM 5-FU with miR-301a and miR-375-3p. Cells transfected with the negative control siRNA are indicated as (–) and GAPDH was used as loading control for each blot.

4 Discussion

Extracellular vesicles (EV), a group of vesicles released from cells either by outward budding or by fusion of multivesicular endosomes (MVE) with the plasma membrane, have become of growing interest in scientific research. Initially thought to serve as intercellular waste collection and removal, their unique and selective packaging as well as their capability to be shuttled and taken up by recipient cells has been shown the importance of extracellular vesicles in intercellular communication. These vesicles are subdivided in two major groups: microvesicles and exosomes. While microvesicles with a size distribution from 100 – 1000 nm, generate by budding from the plasma membrane, exosomes derive from inward budding of early endosomes forming MVE and are released upon fusion of these MVE with the plasma membrane. Their occurrence was shown to be evolutionarily conserved throughout eukaryotic and prokaryotic cells and even in plants. The cargo of extracellular vesicles has been found to include a broad variety of molecules, ranging from DNA, mRNA, miRNA and other small non-coding RNAs, as well as proteins and lipids.(Théry, 2011) (Tkach and Thery, 2016, Schmidt et al., 2004)

The important role of extracellular vesicles in tumourigenesis, progression and metastasis has been observed in the recent decade. The amount of extracellular vesicles secreted from cancer cells is significantly higher compared to normal cells. Also the content and composition of cancer EVs was shown to differ substantially from healthy cells (Azmi et al., 2013). Their impact on the tumour microenvironment was shown in several studies (Haga et al., 2015) (Kahlert and Kalluri, 2013). Furthermore, EVs originated from cancer cells and their content, like specific microRNAs, might be a possibility to serve as biomarkers for multiple cancer types (Roy et al., 2018).

Cancer being one of the most live threatening diseases in modern medicine, has become even more difficult to fight due to the emergence of drug resistances, especially after long-term treatment and exposure to the drugs. The involvement of extracellular vesicles in the process of chemoresistance acquirement has been shown in a number of cancer types, including neuroblastomas (Challagundla et al., 2015) and breast cancer (Chen et al., 2014). The role of microRNAs in chemoresistance has also been shown in multiple tumour types, also in the resistance against 5-fluorouracil in colorectal cancer (Schmidt et al., 2004).

The transfer of 5-FU resistance by EVs was tested by incubation of naïve colorectal cancer cells with EVs isolated from chemoresistant colorectal cancer cells. The influence of this co-cultivation on the chemosensitivity of naïve cell lines was tested by determining shifts in the EC_{50} of 5-FU using MTT assays. After performing multiple experiments at diverse conditions, varying effects of resistant EVs on the chemosensitivity of naïve colorectal cancer cells were observed. The highly 5-FU sensitive cell line CCL 247 and the naïve primary adenoma carcinoma cell line CCL 228 showed no significant change in chemosensitivity when co-cultivated with EVs from resistant colorectal cancer cells. Experiments performed with the cell line CaCo2 and the naive lymph node metastasis cell line CCL 227 resulted in some instances in a significant shift in the EC_{50}. However, these results were highly variable and not consistent throughout the different experiments. The changes in the EC_{50} ranged from a two-fold increase to a decrease by 50%. These variations were only observed in the biological replicates, whereas the technical replicates were clearly reproducible and showed acceptable distribution of the results. A methodological explanation for the contradicting results could be the unsuitability and the limitations of the MTT assay with 5-FU. Most experiments conducted with EVs to test their effects on recipient cells, for example effects on their chemosensitivity, don't exceed an incubation time of 24 to 48 hours (Chen et al., 2014, Challagundla et al., 2015). Yet, conducting MTT assays to determine the EC_{50} and shifts thereof requires an incubation time of recipient cells with EVs of 144 hours, since cells need to be exposed to 5-FU for this period of time before performing the MTT assay (Mader et al., 1997). This should be taken into account and tested in further experiments, for example by repeated addition of EVs throughout the incubation time or by co-culturing naïve colorectal cancer cells repeatedly for a longer period before conducting MTT assays with 5-FU. Furthermore, improving isolation with novel methods and using EVs directly after isolation might reduce the variations in the results. However, one should not only consider the methodological aspects but also the biological ones, which could be responsible for the broad variations. Since resistant cancer cells are thought to produce subpopulations of extracellular vesicles, including also vesicles used as efflux pumps to remove drugs from the cells (Cesi et al., 2016), it could be possible that varying effects on chemoresistance occur due to differences in the composition of isolated EV populations. At present, it is not possible to methodically discriminate and characterize subpopulation and subtypes of EVs (Colombo et al., 2014). The enrichment of drugs in EVs could also explain the observed doubled population doubling time of naïve colorectal cancer cells when incubated with EVs from the high resistant lymph node metastasis cell line, which could also impact results when testing chemosensitivity over time. Lastly, both methodological and biological aspects should be taken into consideration for further experiments investigating the transfer of resistance with EVs.

The inducible NF-κB signalling pathway comprising of transcription factors regulating gene expression was shown to play a vital role in cellular immune response, inflammation, proliferation and apoptosis. The dysregulation of this pathway is thought to be key component of tumorigenesis, tumourprogression and development of chemoresistance (Hoesel and Schmid, 2013). Studying the influence of resistant EVs on the activation of the NF-κB pathway of naïve colorectal cancer cells by incubation thereof with EVs isolated from colorectal cancer cells with progressing degree of resistance, showed no direct activation of the pathway by Western blot. However, the NF-κB signalling pathway is not only triggered by extracellular stimuli, but can also be influenced by microRNAs (Tan et al., 2012). In literature, a vast number of NF-κB influencing microRNAs is described. Twentyseven of the most promising microRNAs suggested by literature were cross-referenced with microarray data from colorectal cancer cell lines. Of the total number of twentyseven microRNAs checked, six showed to be differentially expressed in colorectal cancer cell lines, depending on their level of chemosensitivity, more specifically chemoresistance. The differential expression of these six miRNAs was validated by real time PCR and showed promising results in two cases: miR-301a and miR-375-3p. Their impact on the NF-κB pathway was previously described by Olarerin-George et al (2013) and Mutlu et al (2016). Even though, transfection of naïve colorectal cancer cells with these microRNAs was successful, no clear activation of the NF-κB pathway could be observed by Western blot. However, transfection of the high resistant lymph node metastasis cell line interestingly resulted in selective packaging of miR-375-3p and retention of miR-301a, which could be further investigated. Another aspect one should keep in mind, is that interactions of microRNAs with the NF-κB signalling pathway may be triggered by the combination of several microRNAs.

In summary, no conclusion about the impact of EVs isolated from the supernatant of chemoresistant colorectal cancer cells on the chemosensitivity of naïve colorectal cancer cells regarding the transfer of resistance could be made due to the wide variability in the obtained results. To minimize these variances in future, methodological improvements should be made in EVs isolation, characterisation and in testing the chemosensitivity. The co-cultivation of naïve colorectal cancer cells with EVs from resistant colorectal cancer cells clearly showed no activation of the NF-κB pathway. However, we were able to identify and validate the two miRNAs miR-301a and miR-375-3p, which were differentially expressed in colorectal cancer cells with progressive degrees of chemoresistance against 5-fluorouracil and are thought to have an impact on the NF-κB signaling pathway. Even though we were not able to see an activation of NF-κB by Western blot when cells were transfected with these miRNAs, this could be investigated in more detail by testing, combinations of several microRNAs in further experiments.

The importance of extracellular vesicles in intercellular communication and their high occurrence in and connection to numerous diseases, has led to a growing interest in scientific research. However, this emergent research field is still struggling with the development of standardized methods to study these complex vesicles in more detail (Niel et al., 2018). A deeper understanding of extracellular vesicles, their molecular content and the processes of intercellular communication, they are involved in, is of essential importance to understand their impact and to draw more precise conclusions from accumulating data.

5 Literature

AZMI, A. S., BAO, B. & SARKAR, F. H. 2013. Exosomes in cancer development, metastasis, and drug resistance: a comprehensive review. *Cancer Metastasis Rev,* 32**,** 623-42.

BEBAWY, M., COMBES, V., LEE, E., JAISWAL, R., GONG, J., BONHOURE, A. & GRAU, G. E. 2009. Membrane microparticles mediate transfer of P-glycoprotein to drug sensitive cancer cells. *Leukemia,* 23**,** 1643-9.

BHARTI, A. C. & AGGARWAL, B. B. 2002. Chemopreventive agents induce suppression of nuclear factor-kappaB leading to chemosensitization. *Ann N Y Acad Sci,* 973**,** 392-5.

BRADFORD, M. M. 1976. A rapid and sensitive method for the quantitation of microgram quantities of protein utilizing the principle of protein-dye binding. *Anal Biochem,* 72**,** 248-54.

CESI, G., WALBRECQ, G., MARGUE, C. & KREIS, S. 2016. Transferring intercellular signals and traits between cancer cells: extracellular vesicles as "homing pigeons". *Cell Commun Signal,* 14**,** 13.

CHALLAGUNDLA, K. B., WISE, P. M., NEVIANI, P., CHAVA, H., MURTADHA, M., XU, T., KENNEDY, R., IVAN, C., ZHANG, X., VANNINI, I., FANINI, F., AMADORI, D., CALIN, G. A., HADJIDANIEL, M., SHIMADA, H., JONG, A., SEEGER, R. C., ASGHARZADEH, S., GOLDKORN, A. & FABBRI, M. 2015. Exosome-mediated transfer of microRNAs within the tumor microenvironment and neuroblastoma resistance to chemotherapy. *J Natl Cancer Inst,* 107.

CHEN, W. X., CAI, Y. Q., LV, M. M., CHEN, L., ZHONG, S. L., MA, T. F., ZHAO, J. H. & TANG, J. H. 2014. Exosomes from docetaxel-resistant breast cancer cells alter chemosensitivity by delivering microRNAs. *Tumour Biol,* 35**,** 9649-59.

COLOMBO, M., RAPOSO, G. & THERY, C. 2014. Biogenesis, secretion, and intercellular interactions of exosomes and other extracellular vesicles. *Annu Rev Cell Dev Biol,* 30**,** 255-89.

DE BROE, M., WIEME, R. & ROELS, F. 1975. Letter: Membrane fragments with koinozymic properties released from villous adenoma of the rectum. *Lancet,* 2**,** 1214-5.

FEARON, E. R. & VOGELSTEIN, B. 1990. A genetic model for colorectal tumorigenesis. *Cell,* 61**,** 759-67.

GARDINER, C., DI VIZIO, D., SAHOO, S., THÉRY, C., WITWER, K. W., WAUBEN, M. & HILL, A. F. 2016. Techniques used for the isolation and characterization of extracellular vesicles: results of a worldwide survey. *J Extracell Vesicles,* 5**,** 32945.

GODWIN, P., BAIRD, A. M., HEAVEY, S., BARR, M. P., O'BYRNE, K. J. & GATELY, K. 2013. Targeting nuclear factor-kappa B to overcome resistance to chemotherapy. *Front Oncol,* 3**,** 120.

GYORGY, B., SZABO, T. G., PASZTOI, M., PAL, Z., MISJAK, P., ARADI, B., LASZLO, V., PALLINGER, E., PAP, E., KITTEL, A., NAGY, G., FALUS, A. & BUZAS, E. I. 2011. Membrane vesicles, current state-of-the-art: emerging role of extracellular vesicles. *Cell Mol Life Sci,* 68**,** 2667-88.

HAGA, H., YAN, I. K., TAKAHASHI, K., WOOD, J., ZUBAIR, A. & PATEL, T. 2015. Tumour cell–derived extracellular vesicles interact with mesenchymal stem cells to modulate the microenvironment and enhance cholangiocarcinoma growth. *http://dx.doi.org/10.3402/jev.v4.24900*.

HARDING, C. V., HEUSER, J. E. & STAHL, P. D. 2013. Exosomes: Looking back three decades and into the future.

HAYDEN, M. S. & GHOSH, S. 2008. Shared principles in NF-kappaB signaling. *Cell,* 132**,** 344-62.

HOESEL, B. & SCHMID, J. A. 2013. The complexity of NF-κB signaling in inflammation and cancer. *Mol Cancer,* 12**,** 86.

JOST, P. J. & RULAND, J. 2007. Aberrant NF-kappaB signaling in lymphoma: mechanisms, consequences, and therapeutic implications. *Blood,* 109**,** 2700-7.
KAHLERT, C. & KALLURI, R. 2013. Exosomes in tumor microenvironment influence cancer progression and metastasis. *J Mol Med (Berl),* 91**,** 431-7.
KHARAZIHA, P., CHIOUREAS, D., RUTISHAUSER, D., BALTATZIS, G., LENNARTSSON, L., FONSECA, P., AZIMI, A., HULTENBY, K., ZUBAREV, R., ULLEN, A., YACHNIN, J., NILSSON, S. & PANARETAKIS, T. 2015. Molecular profiling of prostate cancer derived exosomes may reveal a predictive signature for response to docetaxel. *Oncotarget,* 6**,** 21740-54.
KIM, T. K. & EBERWINE, J. H. 2010. Mammalian cell transfection: the present and the future. *Anal Bioanal Chem,* 397**,** 3173-8.
KING, H. W., MICHAEL, M. Z. & GLEADLE, J. M. 2012. Hypoxic enhancement of exosome release by breast cancer cells. *BMC Cancer,* 12**,** 421.
KORBER, M. I., STARIBACHER, A., RATZENBOCK, I., STEGER, G. & MADER, R. M. 2016. NFkappaB-Associated Pathways in Progression of Chemoresistance to 5-Fluorouracil in an In Vitro Model of Colonic Carcinoma. *Anticancer Res,* 36**,** 1631-9.
LI, Y., AHMED, F., ALI, S., PHILIP, P. A., KUCUK, O. & SARKAR, F. H. 2005. Inactivation of nuclear factor kappaB by soy isoflavone genistein contributes to increased apoptosis induced by chemotherapeutic agents in human cancer cells. *Cancer Res,* 65**,** 6934-42.
LIVAK, K. J. & SCHMITTGEN, T. D. 2001. Analysis of relative gene expression data using real-time quantitative PCR and the 2(-Delta Delta C(T)) Method. *Methods,* 25**,** 402-8.
LOGOZZI, M., DE MILITO, A., LUGINI, L., BORGHI, M., CALABRO, L., SPADA, M., PERDICCHIO, M., MARINO, M. L., FEDERICI, C., IESSI, E., BRAMBILLA, D., VENTURI, G., LOZUPONE, F., SANTINAMI, M., HUBER, V., MAIO, M., RIVOLTINI, L. & FAIS, S. 2009. High levels of exosomes expressing CD63 and caveolin-1 in plasma of melanoma patients. *PLoS One,* 4**,** e5219.
LONGLEY, D. B., HARKIN, D. P. & JOHNSTON, P. G. 2003. 5-fluorouracil: mechanisms of action and clinical strategies. *Nat Rev Cancer,* 3**,** 330-8.
MA, X., BECKER BUSCAGLIA, L. E., BARKER, J. R. & LI, Y. 2011. MicroRNAs in NF-kappaB signaling. *J Mol Cell Biol,* 3**,** 159-66.
MADER, R. M., SIEDER, A. E., BRAUN, J., RIZOVSKI, B., KALIPCIYAN, M., MUELLER, M. W., JAKESZ, R., RAINER, H. & STEGER, G. G. 1997. Transcription and activity of 5-fluorouracil converting enzymes in fluoropyrimidine resistance in colon cancer in vitro. *Biochem Pharmacol,* 54**,** 1233-42.
MAHMOOD, T. & YANG, P. C. 2012. Western Blot: Technique, Theory, and Trouble Shooting. *N Am J Med Sci.*
MULCAHY, L. A., PINK, R. C. & CARTER, D. R. F. 2014. Routes and mechanisms of extracellular vesicle uptake. *http://dx.doi.org/10.3402/jev.v3.24641*.
MUTLU, M., RAZA, U., SAATCI, O., EYUPOGLU, E., YURDUSEV, E. & SAHIN, O. 2016. miR-200c: a versatile watchdog in cancer progression, EMT, and drug resistance. *J Mol Med (Berl),* 94**,** 629-44.
NIEL, G. V., D'ANGELO, G. & RAPOSO, G. 2018. Shedding light on the cell biology of extracellular vesicles. *Nature Reviews Molecular Cell Biology,* 19**,** 213.
PFAFFL, M. W. 2001. A new mathematical model for relative quantification in real-time RT-PCR. *Nucleic Acids Res,* 29**,** e45.
QIAGEN 2012. microRNA Sample and Assay Technologies Manual.
RAPOSO, G. & STOORVOGEL, W. 2013. Extracellular vesicles: exosomes, microvesicles, and friends. *J Cell Biol,* 200**,** 373-83.
RIO, D. C., ARES, M., JR., HANNON, G. J. & NILSEN, T. W. 2010. Purification of RNA using TRIzol (TRI reagent). *Cold Spring Harb Protoc,* 2010**,** pdb.prot5439.
RISS, T. L., MORAVEC, R. A., NILES, A. L., DUELLMAN , S., BENINK, H. A., WORZELL , T. J. & MINOR, L. 2013. Cell Viability Assays. *Assay Guidance Manual.*
ROGLER, G. 2014. Chronic ulcerative colitis and colorectal cancer. *Cancer Lett,* 345**,** 235-41.

ROY, S., HOCHBERG, F. H. & JONES, P. S. 2018. Extracellular vesicles: the growth as diagnostics and therapeutics; a survey. *https://doi.org/10.1080/20013078.2018.1438720*.

SCHMIDT, W. M., KALIPCIYAN, M., DORNSTAUDER, E., RIZOVSKI, B., STEGER, G. G., SEDIVY, R., MUELLER, M. W. & MADER, R. M. 2004. Dissecting progressive stages of 5-fluorouracil resistance in vitro using RNA expression profiling. *Int J Cancer,* 112**,** 200-12.

SENFTER, D., HOLZNER, S., KALIPCIYAN, M., STARIBACHER, A., WALZL, A., HUTTARY, N., KRIEGER, S., BRENNER, S., JAGER, W., KRUPITZA, G., DOLZNIG, H. & MADER, R. M. 2015. Loss of miR-200 family in 5-fluorouracil resistant colon cancer drives lymphendothelial invasiveness in vitro. *Hum Mol Genet,* 24**,** 3689-98.

SIEGEL, R. L., MILLER, K. D. & JEMAL, A. 2018. Cancer statistics, 2018. *CA Cancer J Clin,* 68**,** 7-30.

TAN, G., NIU, J., SHI, Y., OUYANG, H. & WU, Z. H. 2012. NF-kappaB-dependent microRNA-125b up-regulation promotes cell survival by targeting p38alpha upon ultraviolet radiation. *J Biol Chem,* 287**,** 33036-47.

THERY, C., AMIGORENA, S., RAPOSO, G. & CLAYTON, A. 2006. Isolation and characterization of exosomes from cell culture supernatants and biological fluids. *Curr Protoc Cell Biol,* Chapter 3**,** Unit 3.22.

THÉRY, C. 2011. Exosomes: secreted vesicles and intercellular communications. *F1000 Biol Rep.*

TKACH, M. & THERY, C. 2016. Communication by Extracellular Vesicles: Where We Are and Where We Need to Go. *Cell,* 164**,** 1226-1232.

TRAMS, E. G., LAUTER, C. J., SALEM, N., JR. & HEINE, U. 1981. Exfoliation of membrane ecto-enzymes in the form of micro-vesicles. *Biochim Biophys Acta,* 645**,** 63-70.

VADLAPATLA, R. K., VADLAPUDI, A. D., PAL, D. & MITRA, A. K. 2013. Mechanisms of drug resistance in cancer chemotherapy: coordinated role and regulation of efflux transporters and metabolizing enzymes. *Curr Pharm Des,* 19**,** 7126-40.

VIATOUR, P., MERVILLE, M. P., BOURS, V. & CHARIOT, A. 2005. Phosphorylation of NF-kappaB and IkappaB proteins: implications in cancer and inflammation. *Trends Biochem Sci,* 30**,** 43-52.

VLASSOV, A., LI, M., ZERINGER, E., CONRAD, R. & CORP, L. T. 2013. *Methods and compositions for exosome isolation*.

YÁÑEZ-MÓ, M., SILJANDER, P. R.-M., ANDREU, Z., ZAVEC, A. B., BORRÀS, F. E., BUZAS, E. I., BUZAS, K., CASAL, E., CAPPELLO, F., CARVALHO, J., COLÁS, E., SILVA, A. C.-D., FAIS, S., FALCON-PEREZ, J. M., GHOBRIAL, I. M., GIEBEL, B., GIMONA, M., GRANER, M., GURSEL, I., GURSEL, M., HEEGAARD, N. H. H., HENDRIX, A., KIERULF, P., KOKUBUN, K., KOSANOVIC, M., KRALJ-IGLIC, V., KRÄMER-ALBERS, E.-M., LAITINEN, S., LÄSSER, C., LENER, T., LIGETI, E., LINĒ, A., LIPPS, G., LLORENTE, A., LÖTVALL, J., MANČEK-KEBER, M., MARCILLA, A., MITTELBRUNN, M., NAZARENKO, I., HOEN, E. N. M. N.-T., NYMAN, T. A., O'DRISCOLL, L., OLIVAN, M., OLIVEIRA, C., PÁLLINGER, É., PORTILLO, H. A. D., REVENTÓS, J., RIGAU, M., ROHDE, E., SAMMAR, M., SÁNCHEZ-MADRID, F., SANTARÉM, N., SCHALLMOSER, K., OSTENFELD, M. S., STOORVOGEL, W., STUKELJ, R., GREIN, S. G. V. D., VASCONCELOS, M. H., WAUBEN, M. H. M. & WEVER, O. D. 2015. Biological properties of extracellular vesicles and their physiological functions. *http://dx.doi.org/10.3402/jev.v4.27066*.

ZHANG, H. C., LIU, X. B., HUANG, S., BI, X. Y., WANG, H. X., XIE, L. X., WANG, Y. Q., CAO, X. F., LV, J., XIAO, F. J., YANG, Y. & GUO, Z. K. 2012. Microvesicles derived from human umbilical cord mesenchymal stem cells stimulated by hypoxia promote angiogenesis both in vitro and in vivo. *Stem Cells Dev,* 21**,** 3289-97.

6 Appendix

Table 26: List of primer for qPCR

Primer	miRNA target sequence 5'-3'	miRBase Accession	Cat. no
Hs_miR-125b_1	UCCCUGAGACCCUAACUUGUGA	MIMAT0000423	MS00006629
Hs_miR-141_1	UAACACUGUCUGGUAAAGAUGG	MIMAT0000432	MS00003507
Hs_miR-200c_1	UAAUACUGCCGGGUAAUGAUGGA	MIMAT0000617	MS00003752
Hs_miR-301a_1	CAGUGCAAUAGUAUUGUCAAAGC	MIMAT0000688	MS00009317
Hs_miR-375_2	UUUGUUCGUUCGGCUCGCGUGA	MIMAT0000728	MS00031829
Hs_miR-429_1	UAAUACUGUCUGGUAAAACCGU	MIMAT0001536	MS00004193
RNU48 (SNORD48)	NR_002745	-	-

Table 27: List of miRNA mimics used for transformation

miRNA Mimic	mature miRNA sequence 5'-3'	Sanger ID	Cat. no
Syn-hsa-miR-375	UUUGUUCGUUCGGCUCGCGUGA	HAS-MIR-375	MSY0000728
Syn-hsa-miR301a_3p	CAGUGCAAUAGUAUUGUCAAAGC	HAS-MIR-301a-3p	MSY0000688

Table 28: Fold changes in expression levels of miR-125-5p. The expression in CCL 227, CCL 227 + 5 µM 5-FU, CCL 227 + 25 µM 5-FU CCL 227 + 125 µM 5-FU cells and extracellular vesicles (EVs) was compared to the expression in respectively lower resistant cells and EVs. Fold changes lower than one signify downregulation, whereas fold changes higher than one signify upregulations.

Fold change of ↓ in comparison to →	CCL 228		CCL 227		CCL 227 + 5 µM 5-FU		CCL 227 + 25 µM 5-FU	
	cells	EVs	cells	EVs	cells	EVs	cells	EVs
CCL 227	3.27	1.83						
CCL 227 + 5 µM 5-FU			1.53	1.06				
CCL 227 + 25 µM 5-FU			1.47	1.86	0.97	1.78		
CCL 227 + 125 µM 5-FU			1.59	1.55			1.06	0.84

Table 29: Fold changes in expression levels of miR-141-3p. The expression in CCL 227, CCL 227 + 5 µM 5-FU, CCL 227 + 25 µM 5-FU CCL 227 + 125 µM 5-FU cells and extracellular vesicles (EVs) was compared to the expression in respectively lower resistant cells and EVs. Fold changes lower than one signify downregulation, whereas fold changes higher than one signify upregulations.

FOLD CHANGE OF ↓ IN COMPARISON TO →	CCL 228		CCL 227		CCL 227 + 5 µM 5-FU		CCL 227 + 25 µM 5-FU	
	CELLS	EVS	CELLS	EVS	CELLS	EVS	CELLS	EVS
CCL 227	0.02	0.25						
CCL 227 + 5 µM 5-FU			0.12	0.17				
CCL 227 + 25 µM 5-FU			0.09	0.16	0.8	0.99		
CCL 227 + 125 µM 5-FU			0.06	0.14			0.66	0.82

Table 30: Fold changes in expression levels of miR-200c-3p. The expression in CCL 227, CCL 227 + 5 µM 5-FU, CCL 227 + 25 µM 5-FU CCL 227 + 125 µM 5-FU cells and extracellular vesicles (EVs) was compared to the expression in respectively lower resistant cells and EVs. Fold changes lower than one signify downregulation, whereas fold changes higher than one signify upregulations.

FOLD CHANGE OF ↓ IN COMPARISON TO →	CCL 228		CCL 227		CCL 227 + 5 µM 5-FU		CCL 227 + 25 µM 5-FU	
	CELLS	EVS	CELLS	EVS	CELLS	EVS	CELLS	EVS
CCL 227	0.26	0.33						
CCL 227 + 5 µM 5-FU			0.40	0.30				
CCL 227 + 25 µM 5-FU			0.54	0.27	1.38	0.94		
CCL 227 + 125 µM 5-FU			0.26	0.32			0.48	1.13

Table 31: Fold changes in expression levels of miR-429-5p. The expression in CCL 227, CCL 227 + 5 µM 5-FU, CCL 227 + 25 µM 5-FU CCL 227 + 125 µM 5-FU cells and extracellular vesicles (EVs) was compared to the expression in respectively lower resistant cells and EVs. Fold changes lower than one signify downregulation, whereas fold changes higher than one signify upregulations.

FOLD CHANGE OF ↓ IN COMPARISON TO →	CCL 228		CCL 227		CCL 227 + 5 µM 5-FU		CCL 227 + 25 µM 5-FU	
	CELLS	EVS	CELLS	EVS	CELLS	EVS	CELLS	EVS
CCL 227	0.57	0.85						
CCL 227 + 5 µM 5-FU			0.99	0.35				
CCL 227 + 25 µM 5-FU			0.56	0.35	0.56	0.89		
CCL 227 + 125 µM 5-FU			0.23	0.34			0.39	1.05

7 List of figures

8 List of tables